NUREG/CR-1473

The Wake and Diffusion Structure Behind a Model Industrial Complex

Prepared by K. M. Kothari, J. A. Peterka, R. N. Meroney

Department of Civil Engineering
Colorado State University

Prepared for
U.S. Nuclear Regulatory
Commission

Available from

GPO Sales Program
Division of Technical Information and Document Control
U. S. Nuclear Regulatory Commission
Washington, D. C. 20555

Printed copy price: $4.50

and

National Technical Information Service
Springfield, Virginia 22161

NUREG/CR-1473
RB, R6

The Wake and Diffusion Structure Behind a Model Industrial Complex

Manuscript Completed: October 1981
Date Published: November 1981

Prepared by
K. M. Kothari, J. A. Peterka, R. N. Meroney

Department of Civil Engineering
Colorado State University
Fort Collins, CO 80523

Prepared for
Division of Health, Siting and Waste Management
Office of Nuclear Regulatory Research
U.S. Nuclear Regulatory Commission
Washington, D.C. 20555
NRC FIN B5829
Under Contract No. NRC 04-76-236

Availability of Reference Materials Cited in NRC Publications

Most documents cited in NRC publications will be available from one of the following sources:

1. The NRC Public Document Room, 1717 H Street., N.W.
   Washington, DC 20555
2. The NRC/GPO Sales Program, U.S. Nuclear Regulatory Commission,
   Washington, DC 20555
3. The National Technical Information Service, Springfield, VA 22161

Although the listing that follows represents the majority of documents cited in NRC publications, it is not intended to be exhaustive.

Referenced documents available for inspection and copying for a fee from the NRC Public Document Room include NRC correspondence and internal NRC memoranda; NRC Office of Inspection and Enforcement bulletins, circulars, information notices, inspection and investigation notices; Licensee Event Reports; vendor reports and correspondence; Commission papers; and applicant and licensee documents and correspondence.

The following documents in the NUREG series are available for purchase from the NRC/GPO Sales Program: formal NRC staff and contractor reports, NRC-sponsored conference proceedings, and NRC booklets and brochures. Also available are Regulatory Guides, NRC regulations in the *Code of Federal Regulations*, and *Nuclear Regulatory Commission Issuances*.

Documents available from the National Technical Information Service include NUREG series reports and technical reports prepared by other federal agencies and reports prepared by the Atomic Energy Commission, forerunner agency to the Nuclear Regulatory Commission.

Documents available from public and special technical libraries include all open literature items, such as books, journal and periodical articles, transactions, and codes and standards. *Federal Register* notices, federal and state legislation, and congressional reports can usually be obtained from these libraries.

Documents such as theses, dissertations, foreign reports and translations, and non-NRC conference proceedings are available for purchase from the organization sponsoring the publication cited.

Single copies of NRC draft reports are available free upon written request to the Division of Technical Information and Document Control, U.S. Nuclear Regulatory Commission, Washington, DC 20555.

ABSTRACT

THE WAKE AND DIFFUSION STRUCTURE BEHIND
A MODEL INDUSTRIAL COMPLEX

The mean velocity, turbulence intensity and turbulent diffusion behind a model of the EOCR complex deeply submerged in a neutral turbulent boundary layer, have been investigated using wind-tunnel tests and mathematical analysis. The effects of the momentum-type wake behind a complex are to decrease mean velocity and increase turbulence intensity. The complex geometry breaks down the horseshoe vortices, which consequently do not play an important role in determining wake characteristics. The decay rate of mean velocity defect was smaller than that of turbulence intensity excess variance. The wake was detected at a distance of x/H equal to 35 at a 5 percent mean velocity defect level. Such long wake regions are associated with the low roughness characteristics of the site.

The vertical profiles of velocity defect and maximum velocity defect rates compared very well with the analytical predictions except at y/H = -0.67. The experimental measurements of the decay rate of turbulence intensity excess variance also compared very well with that predicted by the theory. The ground-level concentration compared satisfactorily with the perturbation theory.

TABLE OF CONTENTS

LIST OF FIGURES

LIST OF FIGURES (CONTINUED)

LIST OF SYMBOLS

Symbol	Definition
A,B,C	calibration constant for hot films
a	virtual origin of wake
C	concentration in the absence of the EOCR complex
C_{Fx},C_{Fy},C_{Fz}	force coefficients of the EOCR complex in x, y, and z directions
C_0,C_2	functions used in Equation [1.5]
C_w	concentration in the wake of the EOCR complex
c	perturbation in concentration due to the EOCR complex
Delta U	mean velocity defect in the wake of the EOCR complex
Delta Var	turbulence intensity excess variance
E	mean output voltage of constant-temperature hot-wire anemometer
F_x,F_y,F_z	forces in x, y, and z directions
H	height of the EOCR reactor building
h	stack height
I_j	modified Bessel's function of integer order j
k	von Karman constant
k_1	constant defined in Equation [1.2]
k_3	constant defined in Equation [1.5]
n	mean velocity power law exponent
$\bar{U}$,$\bar{V}$,$\bar{W}$	mean velocity components in x, y, and z directions
$\bar{U}_w$,$\bar{V}_w$,$\bar{W}_w$	mean velocity components in x, y, and z directions in the wake of the EOCR complex
u,v,w	perturbations of mean velocity components in x, y, and z directions in the wake of the EOCR complex
U_{rms}	root-mean-square of velocity fluctuations
W	width of the complex
x,y,z	space co-ordinates: x, downwind; y, lateral; z, vertical

LIST OF SYMBOLS (CONTINUED)

Symbol	Direction
x', z'	nondimensional space coordinates
z_o	roughness height
$\bar{\nu}$	mean eddy viscosity
$\bar{\nu}_1, \bar{\nu}_2, \bar{\nu}_3$	mean eddy viscosity in x, y, and z directions
γ, λ	constants of order one
δ	boundary layer thickness

ACKNOWLEDGEMENTS

This research was conducted under contract No. AT(49-24)-0366 with the United States Nuclear Regulatory Commission, Office of Nuclear Regulatory Research. Financial support received is gratefully acknowledged. The authors also thank Dr. Robert Abbey, Jr., NRC, for the helpful suggestions and encouragement during the course of the research.

Chapter I

INTRODUCTION AND REVIEW

1.1 Introduction

This report presents a study of the wake and turbulent diffusion behind an industrial complex deeply immersed in a neutral turbulent boundary layer. The purpose of the study was to compare the wake behavior of an idealized model building with the actual industrial complex and compare pollutant diffusion measurements against a new perturbation method.

A surface obstacle or building in the planetary boundary layer creates a wake behind the obstacle. The wake is generally characterized by increased turbulence intensity and decreased mean longitudinal velocity. The loss of velocity in the wake amounts to loss of momentum. The moment of the loss of momentum is then related to the couple acting on the obstacle. An obstacle wake dominated by this effect is known as a momentum wake or normal wake. Passage of a shear flow around a surface obstacle also creates a system of longitudinal vortices in the wake of the obstacle. These vortices bring higher-momentum, less-turbulent fluid from higher elevations of the turbulent boundary layer to increase the velocity and decrease the turbulent intensity close to the surface near the wake centerline. However, the vortices also bring lower-momentum, high-turbulent fluid from the lower elevation of the turbulent boundary layer to decrease velocity and increase turbulence intensity above ground level on the outboard side of the vortices. An obstacle wake dominated by this phenomenon is classified as a vortex wake.

Diffusion of material released in the wake of an industrial complex will be strongly altered as compared with unobstructed terrain, particularly if the pollutant is released within the separation bubble

in the lee of a building. Modeling the pollutant concentration in the wake of the building requires the knowledge of flow characteristics within the wake. For example, using the data of Peterka and Cermak (1975) for decay rate of excess turbulent intensity, Huber and Snyder (1976) developed a prediction technique for pollutant concentration in building wakes. Another area in which knowledge of building wakes is important is the effect of nearby buildings on the wind load requirement of a structure. Zambrano and Peterka (1978) have carried out an extensive study to determine the pressure loading on a building due to an adjacent building. Also, pedestrian comfort near buildings is frequently influenced by the wake characteristics of a building.

1:200 scale models of the EOCR reactor building and surrounding silo and tank buildings at the Idaho National Engineering Laboratory, Idaho Falls, Idaho were put into the Industrial Aerodynamic Wind Tunnel at Colorado State University to determine the wake structure of the complex. Turbulent diffusion around the same complex is discussed in the report by Hatcher et al. (1977). It was expected that with surrounding buildings the horseshoe vortices due to the main EOCR reactor building would degenerate. Therefore, the wake structure of the EOCR complex will be examined in terms of momentum wake theory.

1.2 Building Wakes

1.2.1 Prototype Measurements

High cost, limited data acquisition ability, and the nonstationary character of the atmosphere have severely limited the availability of prototype measurements. Two extensive sets of prototype measurements have been reported; one by Colmer (1971) in the wake of a hanger at the Royal Aircraft Establishment at Bedford, England, and another by Frost

and Shahabi (1977) behind rectangular buildings at NASA Marshall Space Flight Center at Huntsville, Alabama. Colwer (1971) found that the mean longitudinal speed in the wake was smaller than that in approach flow at the same height. He also reported that the mean velocity wake disappeared by 15 building heights downstream, but the turbulence intensity wake was observed even at 23 heights downstream of the hanger. In Frost and Shahabi's (1977) experiments the mean velocity defect behind a larger building decayed with distance at a rate proportional to $x^{-1.5}$, which agrees with wind-tunnel measurements of Woo, Peterka and Cermak (1976) and theory of Hunt and Smith (1969). However, the extent of the cavity region was somewhere between 11 and 15 H in Frost and Shahabi's measurement versus 5.5 to 7.5 H in Woo et al's experiment.

1.2.2 Wind-Tunnel Measurements

The first intensive laboratory measurements of building wakes were conducted by Counihan (1971). He measured mean velocity, fluctuating velocity and spectra in the wakes of a two-dimensional fence and a cube in a simulated turbulent boundary layer. He found that the velocity defect, the difference between mean velocity in the approach flow and in the wake of a building at the same height, decay rate for the two-dimensional fence was smaller than that of the cube. The scales of turbulence detected were smaller in the wake region than in the approach boundary layer.

Lemberg's (1973) experimental wake data behind several buildings show that the velocity defect decayed at a rate proportional to $x^{-1.58}$, agreeing with Hunt's (1971) theoretical prediction. However, the decay rate of turbulence intensity variance excess, the difference between turbulence intensity variance in the wake of a building and in approach

flow at the same height, was much slower and varied from $x^{-0.11}$ to $x^{-0.30}$. Hunt's (1971) theory predicts this decay rate to be $x^{-2.0}$.

Kothari, Peterka, and Meroney (1979a) performed extensive measurements behind several buildings deeply submerged in a stably stratified turbulent boundary layer. They developed an analytical technique to predict mean velocity and temperature in the wake of a building using combined momentum and vortex wake theories. With stable flow, horseshoe vortices were observed up to sixty heights downstream of the building, resulting in excess mean velocity in far wake and excess temperature in the wake.

1.2.3 Theoretical and Numerical Methods

A theoretical foundation for wake behavior behind bluff bodies immersed in a thick turbulent boundary layer was pioneered by Hunt and Smith (1969). They proposed a theory to calculate time-mean velocity in the wake of two- and three-dimensional bluff bodies immersed in a thick turbulent boundary layer. The momentum wake theory of Hunt and Smith is based on the assumption that only small perturbations to the turbulent boundary layer are caused by the obstacle, that the ratio of the model height to the boundary layer height is very small, and that velocity defects in the wake are small compared with the mean longitudinal velocity. The theory is valid only for the far wake region, because the separated region behind the model cannot be considered to be a small perturbation on the approach flow. This theory also assumes a power-law profile for approach flow mean velocity, with power-law exponent $n << 1$. The mean velocities in the wake were expressed in terms of perturbations to the undisturbed flow:

$$\bar{U}_w = \bar{U}(x, z) + u(x, y, z),$$

$$\bar{V}_w = v(x, y, z), \text{ and} \qquad [1.1]$$

$$\bar{W}_w = w(x, y, z),$$

where $\bar{U}$ is the mean velocity in the approach flow, $\bar{U}_w$, $\bar{V}_w$, $\bar{W}_w$, u, v and w are the mean velocities and perturbation velocities in the x, y and z directions, respectively, in the building wake (see Figure 1). The assumption that u, v and w vanish as $x \to \infty$ implies that farther downstream the effect of the building disappears, and the flow field returns to the approach conditions.

For the two-dimensional obstacle case, an empirical relationship was used by Hunt and Smith (1969) to obtain the perturbation shear stress for closure of the equations of motion. From this, an equation for eddy viscosity was derived. The equation for eddy viscosity was integrated across the boundary layer using the approach flow condition to estimate an average eddy viscosity, $\bar{\nu} = 2K^2 nH\bar{U}(H)/(2+n)$. k and n are the von Karman constant and the power-law profile exponent in the approach flow respectively. For the three-dimensional obstacle case, the constant eddy viscosities, $\bar{\nu}_2$ and $\bar{\nu}_3$ in y and z directions respectively, were then approximated by $\bar{\nu}_3 = \gamma\bar{\nu}$ and $\bar{\nu}_2 = \lambda\bar{\nu}_3 = \lambda\gamma\bar{\nu}$; λ and γ are constants of order one. Using this approximation, the turbulent shear stresses τ_{xz} and τ_{xy} are expressed as $\tau_{xz} = \bar{\nu}_3 \frac{\partial \bar{U}}{\partial z}$ and $\tau_{xy} = \bar{\nu}_2 \frac{\partial \bar{U}}{\partial y}$. Assuming a Gaussian distribution of velocity defect in the lateral directions, the first-order solution of the equation of motion was obtained by Hunt and Smith (1969).

The three-dimensional wake solution can be summarized:

$$\frac{u(x, y, z)}{\bar{U}(H)} = k_1 F_1(z'', y'')/[(x - a)/H]^{\frac{3+n}{2+n}} \qquad [1.2]$$

where $u(x, y, z)$ = velocity defect,

$\bar{U}(H)$ = velocity at building height H in the undisturbed flow,

a = virtual origin of the wake, to be determined from experiment,

n = boundary layer velocity profile power-law exponent,

$$k_1 = 0.21\, C_{Fx}\, (W/H)/\{4\lambda^{1/2}\, \gamma(2K^2 n/(2+n))^{\frac{3+n}{2+n}}\},$$

W = width of building,

λ and γ = constants of order one that are adjusted to give optimum agreement between theoretical and experimental results,

k = von Karman constant = 0.41,

C_{Fx} = force coefficient on building,

$$F_1(z'', y'') = \frac{\eta^{\frac{1}{2+n}} \mathrm{Exp}[-(\eta + y''^2/(1.5 + \eta))]}{(\eta + 1.5)^{1/2}},$$

$$z'' = (z/H)/[(x - a)/H]^{\frac{1}{2+n}},$$

$$\eta = z''^{(2+n)}/[2(2 + n)\, K^2 n\, \gamma],$$

$$y'' = \frac{(y/H)}{[(x - a)/H]^{\frac{1}{(2+n)}}} \left[\frac{2+n}{2\lambda\gamma K^2 n}\right]^{\frac{1}{(2+n)}}.$$

Similar results are available for the two-dimensional case. The perturbation fluctuating velocity was also determined. Briefly, for the three-dimensional case, the mean square longitudinal fluctuating velocity varies as $\Delta u^2_{rms}/\bar{U}(H)^2 \cong 1.0/(x/H)^2$ and the two-dimensional case varies as $\Delta u^2_{rms}/\bar{U}(H)^2 \cong 10.0\, (K^2 n)^{1/2}/(x/H)^{3/2}$.

Hunt's theory provides a method to plot the experimental data in a universal form. For a three-dimensional case the experimental data can be plotted as $\left(u/\bar{U}(H)\right)\left(\frac{x-a}{H}\right)^{(3+n)/(2+n)}$ against $(z/H)/\left(\frac{x-a}{H}\right)^{1/(2+n)}$ to give a universal curve. For n small, Hunt's momentum theory predicts that the mean velocity defect decays approximately as $x^{-3/2}$.

Hunt (1971) compared the above momentum wake theory with the results of Counihan (1971). For a two-dimensional block, Counihan found that the mean velocity defect decayed as $x^{-0.47}$, whereas Hunt predicted a mean velocity defect decay rate of $x^{-1.0}$. Hunt attributed the difference to his assumption of constant eddy viscosity; however, the experimental values of the mean velocities behind the cube did fit a universal curve as suggested by Hunt's theory.

Lemberg (1973) recognized the weakness of the constant eddy viscosity assumption in Hunt's theory. Lemberg assumed a variable viscosity of the form $\bar{\nu}_3 = K' z^b H \bar{U}(H)$, where K' and b are arbitrary constants determined by comparison with experimental data. He also assumed the eddy viscosity in the y direction to be proportional to $\bar{\nu}_3$ and has a form of $\bar{\nu}_2 = \bar{\nu}_3 (W/H)^2$, where W and H are the width and height of building. Lemberg determined the value of b to be equivalent to the boundary layer power-law exponent n. Hence, the eddy viscosity used by Lemberg was proportional to the mean longitudinal velocity at the same height in the undisturbed flow. The introduction of variable eddy viscosity did not provide a significant improvement in ability of the theory to match experiments.

Both Lemberg (1973) and Hunt (1971) assumed a Gaussian distribution of mean velocity defect for the lateral direction. However, measurements

by Peterka and Cermak (1975) do not support this hypothesis. They observed in horizontal profiles of mean velocity defect that the profile maxima did not occur on the centerline near the model but were displaced from 1/2 and 1 building width to the side. The displaced maxima were short lived in downstream distance. An interesting feature of the profiles is a secondary peak which occurred 2 to 3 building half-width off the centerline and was observed from 2 to 12-14 H downwind. Similar effects were observed by Hansen, Peterka, and Cermak (1975) in the wake of a rectangular building in a simulated atmosphere boundary layer wind. Peterka and Cermak (1975) concluded that this effect was the result of the well-known horseshoe vortex, which was not considered in Hunt's theory.

Noting the results of Peterka and Cermak (1975), Hunt (1975) developed a small perturbation theory (to be published) for the effect of vortices on wakes behind buildings deeply immersed in the planetary boundary layer. The qualitative view of the flow around a bluff body immersed in a turbulent boundary layer is shown in Figure 1 to illustrate the effect of such a horseshoe vortex. Figure 2 is derived from Hunt's vortex wake theory to show the regions of influence of the vortex cores. The region is divided into three regions: (i) E, where the flow is assumed to be inviscid, (ii) V_+ (and its image V_-), the viscous region surrounding the vortex where there is a balance between Reynolds stress and inertial forces, and (iii) G, where the boundary layer assumptions apply. The growth rates of all these regions were estimated by Hunt, and he concluded that downstream all three regions merge together. This means that the vortex core radius is much larger than the height of the building.

Hunt's theory considers the interaction of a line vortex with the mean vertical velocity shear. It is conceptually similar to the momentum wake theory. The vortex transports higher-momentum fluid from a higher elevation to a lower elevation of the turbulent boundary layer and thus increases the velocity on the inboard side of the vortex. The horseshoe vortex forms in the stagnation region in front of the building and curls around the building to produce a mean vorticity with its axis in the longitudinal direction. The total solution of the multiple vortex system can be obtained by superimposing the result of each vortex in the system. The resultant equations of motion are linear in the perturbation quantities; hence, the solution of momentum wake and vortex wake can also be superimposed.

The exact solution of the equations of motion for Hunt's vortex wake solution in terms of perturbation quantities involves triple integrals which have not yet been evaluated. At present, only the asymptotic results are available for determining the effect of vortices. Hunt has determined that the swirl velocity component decreases as $x^{-1/2}$ when the three regions are distinct, but farther downstream where all three regions merge together, it decreases as x^{-1}. Hunt has also calculated the asymptotic results for the regions V_+ and V_-, and found that the longitudinal perturbation velocity excess induced by a vortex increases as $x^{1/2}$ until the three regions are distinct. Thereafter, Hunt has indicated (not calculated) that the asymptotic solution for longitudinal perturbation velocity excess will be proportional to $x^{-1/2}$.

The longitudinal velocity excess in region E was determined by Hunt and given by,

$$u = \frac{n\Gamma}{\pi} hy'x \left\{ \frac{1}{(y'^2 + h^2 + z^2)^2 - 4z^2h^2} \right\} \qquad [1.3]$$

where $y' = y_v - y$. y_v and h are the locations of the vortex center in lateral and vertical directions respectively and Γ is the circulation at $x = 0$. An interesting feature of the equation [1.3] is that u increases linearly with x in region E; however, this process cannot persist indefinitely. Hunt has concluded that u ceases to vary linearly as soon as the width of the viscous core is approximately equal to y or the depth of the region G equals z.

Hansen and Cermak (1975) have investigated the effect of horseshoe vortices. The velocity perturbation predicted by Equation 1.3 was doubled to account for the two horseshoe vortices observed, one on each side of the hemisphere. In their work, the result that u is proportional to x is clearly noticeable. The theoretical and experimental results are in fair agreement at $x/R = 8.73$. The comparison deteriorates for large x/R ratios due to the assumption of a continuous increase in u. Hunt's theory requires the strength and position of the vortex, the measurements of which are not always available.

Kothari, Peterka, and Cermak (1979b) have proposed to calculate time mean concentration in the wake of a three-dimensional body deeply immersed in a thick turbulent boundary layer. The theory is based on the assumption that only small perturbations in pollutant concentration are caused by the obstacle. The theory also assumes the velocity profile power-law exponent $n << 1$. The mean concentrations in the wake are expressed by

$$C_w = C(x,y,z) + c(x,y,z) \quad , \qquad [1.4]$$

where $C(x,y,z)$ is the mean concentration without obstacle and $c(x,y,z)$ is the perturbation caused by obstacle. The assumption that c vanishes as $x \to \infty$ implies that farther downstream the effect of the obstacle disappears and the concentration distribution approaches to the no-obstacle conditions.

The procedur · utilized for obtaining the solution of perturbation quantity, c, is described in detail by Kothari, Peterka and Meroney (1979b) and is similar to that of Smith (1957). The wake concentration solution is given by:

$$C_w = k_3 \, P(x,z) \, \exp(-y^2/f(x,z)) \qquad [1.5]$$

where

$$f(x,z) = 2C_2/C_o \quad ,$$

$$P(x,z) = C_o \sqrt{C_o/(2\pi C_2)} \quad ,$$

$$C_o = \frac{(1+z')^{n/2}}{(1+2n)\,x'} \exp\left[- \frac{(1+(1+z')^{1+2n})}{(1+2n)^2\,x'} \right] \cdot I_{-n/(1+2n)}\left[\frac{2(1+z')^{(\frac{1+2n}{2})}}{x'(1+2n)^2} \right] ,$$

$$C_2 = \frac{x'}{3} \exp(-\xi) \left[(1+2\xi)\, I_o(\rho) + \rho I_1(\rho) \right] ,$$

$$\xi = \frac{2+z'}{x'} \quad ,$$

$$\rho = \frac{2\sqrt{1+z'}}{x'} \quad ,$$

$$z' = z/h \quad ,$$

$$x' = 2\left(\frac{x}{H}\right)\left(\frac{H}{h}\right)\frac{2nK^2}{(2+n)} \quad ,$$

k_3 = constant to be determined from experiments,

h = stack height,

H = building height,

k = von Karman constant (0.41),

$I_{-n/(1+2n)}$ = modified Bessel function of fractional order,

I_o, I_1 = modified Bessel function of integer order.

Since $n<<1$, $\frac{n}{1+2n}$ is small and so $I_{-n/(1+2n)}$ was equated as I_0. The functions I_0 and I_1 were evaluated using expansion functions from Abramowitz and Stegun (1968). The functions are given by:

$$I_0(t') = 1 + 3.5156t^2 + 3.0899t^4 ,$$

$$I_1(t') = t'[0.5 + 0.8789t^2 + 0.51498t^4] \qquad [1.6]$$

when

$$t = t'/3.75 \quad \text{and} \quad -3.75 \leq t' \leq 3.75 ,$$

and

$$I_0(t') = \frac{1}{\sqrt{t'}} e^{t'} [0.39894 + 0.01328/t] ,$$

$$I_1(t') = \frac{1}{\sqrt{t'}} e^{t'} [0.39894 - 0.03988/t]$$

when

$$3.75 < |t'| .$$

Equation [1.5] with Equation [1.6] should be used for elevated releases only. The ground release prediction for concentration distribution in the wake of a building is described by Kothari, Peterka, and Meroney (1979b).

Kothari, Peterka and Meroney (1979a) have utilized the momentum and vortex wake theories of Hunt. The experimental measurement of velocity defect shows good comparison with the theories of Hunt and Smith (1969) and Hunt (1975). The similar theory developed by Kothari, Peterka, and Meroney (1979a) for mean temperature in the wake of a building submerged in a stably stratified turbulent boundary layer shows excellent comparison with their measurements.

Chapter II

DATA ACQUISITION AND ANALYSIS

This chapter describes the main requirements for wind-tunnel modeling of the building complex, the experimental equipment for velocity and pressure measurement, and the geometry of the modeled complex.

2.1 Wind-Tunnel Boundary Layer Similarity

The boundary layer simulation criteria have been discussed in detail by Cermak (1975), Cermak and Arya (1970), and Snyder (1972, 1979). Requirements sufficient for this research are as follows:

1. Geometric similarity: This can be achieved by undistorted scaling of geometry of the prototype complex in the model complex.
2. Boundary condition similarity: Kinematical similarity can be achieved by accurately modeling the approach flow characteristics. The scaled approach flow mean velocity profile and turbulence characteristics should be the same for model and prototype. The effective surface roughness, turbulence integral scale and boundary-layer depth should be scaled by a reference length.
3. Reynolds number equality: Equal Reynolds numbers are not attainable for model and prototype. However, this does not seriously limit capabilities for modeling atmospheric flow, as the significant flow characteristics are only weakly dependent upon large Reynolds number ($> 2 \times 10^4$) as shown by Schlichting (1979). For the present data, the typical Reynolds number was 1.2×10^5 based on velocity at the height of building.

4. Rossby number equality: For investigation of localized flow characteristics behind a surface obstacle, Coriolis effects are not important; hence, Rossby number equality is not necessary.

Neutral atmospheric boundary layer flows can be modeled by satisfying the above criteria.

2.2 The Wind-Tunnel Facility

The EOCR wake measurements were performed in the Industrial Aerodynamics Wind Tunnel (Figure 3) located in the Fluid Dynamics and Diffusion Laboratory at Colorado State University.

The wind tunnel is a closed-circuit facility driven by a 75 H.P. single-speed induction motor. A 16-blade variablepitch axial fan provides control of the speed in the wind tunnel. The contraction ratio at the entrance of the test section is 4:1. The square cross section of the tunnel is 3.3 m^2 and the length of the test section is 18.3 m. The roof of the last 7.5 m of the test section is adjustable to obtain zero pressure gradient along the test section. Available section velocities range from 0 to 24.4 m/sec. All of the wake data reported in this report were taken at a nominal velocity of 16.7 m/sec. The long test section, in conjunction with spires and a barrier at the entrance, were used to generate a thick turbulent boundary layer simulating a typical neutral boundary layer existing at the EOCR site. The measurements in this report were made at 9.5 m from the test section entrance, where a similarity profile was obtained. The velocity defects were calculated by finding the differences between the velocity at a point in the absence of the model complex and the velocity at the same point in the wake.

2.3 Velocity Measurements

Measurements of mean velocity and turbulence intensity can be accomplished with a single hot-wire anemometer mounted with its axis horizontal. The instrument used was a Thermo Systems constant temperature hot-wire anemometer model 1050 with a 2.54×10^{-3} cm diameter platinum film sensing element 0.0508 cm long. Output from the anemometer was fed to a DISA RMS meter model 55D35 to determine rms voltage. The outputs from the rms meter and raw anemometer were fed to two time constant averaging circuits, and were averaged for 10 seconds with a 10-second time constant set into the circuit, followed by 20 seconds of averaging with a 30-second time constant, followed by 60 seconds of averaging with a 100-second time constant. This sequence of time constants acting on the signal provided a precise and accurate measure of both mean and rms anemometer voltage. Outputs from the averaging circuits were read from digital voltmeters and recorded.

Calibration of the hot-film anemometer was performed daily using a Thermo Systems calibrator model 1125. The calibration data were fit to a variable exponent King's law relationship

$$\bar{E}^2 = A + B\bar{U}^n \qquad [2.1]$$

where $\bar{E}$ = mean hot-film output voltage

$\bar{U}$ = mean velocity

A,B,n = coefficients selected by least square to fit the calibration data

It was not practical to calibrate the hot film in air at the same temperature as the air in the tunnel test section. In addition, the temperature in the wind-tunnel test section normally increased slowly while the tunnel was operating. To correct for the difference between the calibration temperature and the temperature in the tunnel at the

time of the measurement, the method of Bearman (1970) was used. In order to utilize such a correction, temperature differences must be small (< 12°C) and wind speeds should be greater than 0.9 to 1.5 m/sec. Both of these conditions were met in all of the wake measurements. Once the temperature correction to the mean hot-film voltage is obtained, the mean velocity can be extracted using Equation 2.1.

The root-mean-square velocity, U_{rms}, was obtained from (see Sandborn, 1972)

$$U_{rms} = \frac{2\bar{E}\, E_{rms}}{Bn\, \bar{U}^{n-1}} \qquad [2.2]$$

where $\bar{E}$ = corrected mean hot-film voltage

E_{rms} = root-mean-square voltage of hot-film anemometer

The mean velocity defect, Delta U, and turbulence excess, Delta Variance, were determined from

$$\text{Delta } U = \left(\frac{\bar{U}(z)}{\bar{U}(\delta)}\right)_{\text{without model}} - \left(\frac{\bar{U}(z)}{\bar{U}(\delta)}\right)_{\text{with model}}$$

and

$$\text{Delta Variance} = \left(\frac{U_{rms}(z)}{\bar{U}(z)}\right)^2_{\text{with model}} - \left(\frac{U_{rms}(z)}{\bar{U}(z)}\right)^2_{\text{without model}}$$

where $\bar{U}(z)$ and $U_{rms}(z)$ are the mean and rms velocities at elevation z above the surface at a given measurement location and $\bar{U}(\delta)$ is the mean velocity at the outer edge of the turbulent boundary layer.

A newly developed hot-film anemometer technique utilizing a rotating hot film was used to measure the mean velocity vector and the six components of Reynolds stress in the turbulent flow. This rotating

hot-film anemometer system uses the same principles and analysis used for any other yawed sensor. The hot-film is yawed to the flow and then rotated about its probe support axis, varying the angle of flow incidence. By using simple geometrical considerations, information about the magnitude and direction of the mean velocity vector can be extracted from the measurements. Theoretically, the sensor would only have to be rotated to three different angles to determine the mean velocity vector. However, by rotating the film to more than three angles and applying a least-square technique, the bestfit solution to the equation for the mean velocity components can be obtained. The three mean velocity components can then be used in the hot-film anemometer response equation for turbulent flow to obtain the values of the six components of the velocity correlations. There again, six different angular positions of the film would be sufficient to calculate the velocity correlations. However, the best fit solution to the equation can be obtained by rotating the sensor to more than six angular positions and applying the method of least-squares. The details of the measurement technique were described by Marsh and Peterka (1977).

A mechanical traverse with a travel distance of 1.3 m was used to remotely position the transducer at the desired location. The traverse could also be moved manually to other locations in the tunnel. The traverse could be positioned within $\pm$ 3.0 x 10^{-4} m in its direction of travel.

2.4 Pressure Measurements

A Systems Development Inc. digital data acquisition system was used for the measurement of pressure on the complex faces. The important components of the system consist of an 72-channel pressure-selector switch, a strain-gage differential pressure transducer, and a

minicomputer/analog-to-digital converter system. A block diagram for the system is shown in Figure 4. The instantaneous pressure at a location of the model complex was transmitted from the top to the pressure-selector valve through a short section of tubing. The base of the selector valve contained four differential pressure transducers. The pressure from the tap location on the model complex on the building was connected to the positive side of the transducer. The static pressure measured in the free stream above the turbulent boundary layer was connected to the negative side of the transducer. The pressure difference corresponds to the difference between the pressure on the building and local atmospheric pressure. The voltage output of the transducer was a fluctuating d.c. signal. It was fed to an amplifier and then to the analog-to-digital converter.

The analog-to-digital converter, mini-computer and digital tape unit are an integrated system and controlled through a teletype. The pressure signals were sampled at 240 samples/sec and recorded digitally on a magnetic tape for 16.3 sec. The digital tapes data were reduced on the Colorado State University CDC 6400 computer. The sampled voltages were then converted to fluctuating pressures from which mean, maximum, and minimum pressure were calculated for each tap location on the building. The drag on the body was then evaluated for each building in the model complex.

2.5 Description of the Industrial Complex and Test Program

A 1:200 scale model of the EOCR reactor and nearby silo and tank building at the Idaho National Engineering Laboratory, Idaho Falls, Idaho were constructed from Plexiglas and placed in the Industrial Aerodynamics Wind Tunnel at Colorado State University.

Detailed wake measurements for one wind direction (135°), with one face of the reactor building normal to the flow direction, were obtained rather than a series of less detailed measurements at many wind directions. The characteristics of the building wake were measured at various x/H, y/H and z/H locations, as shown in Figure 5. All measurements of velocity were made with and without the complex in place at all locations. The diffusion results reported herein were obtained from Hatcher et al. (1977) for comparison to the present analytical model.

Chapter III

RESULTS AND DISCUSSION

Wind-tunnel measurements of mean and turbulent velocity in the wake of the EOCR complex deeply submerged in a neutral turbulent boundary layer were performed, and are reported in this chapter. Mean velocity measurements and comparison with the momentum wake theory, described in Chapter I, are presented in the first part of the chapter, and the turbulence statistics in the second part of this chapter. The diffusion measurements are compared to the theory at the end of the chapter.

3.1 Approach Flow Characteristics

The approach profile characteristic of the flat area surrounding the EOCR complex was simulated using spires and barriers at the front of the test section and over the flat wind-tunnel floor. The mean velocity and turbulence intensity profiles measured, as described in Chapter II, are shown in Figure 6. The boundary layer thickness, δ, was 1.22 m corresponding to a prototype value of approximately 240 m height. In the form,

$$\frac{\bar{U}(z)}{\bar{U}(\delta)} = \left(\frac{z}{\delta}\right)^{n} \quad , \qquad [3.1]$$

the experimental approach flow velocity profile had an exponent of 0.12 which is an acceptable value for the flat terrain surrounding the EOCR site. If the upstream profile shown in Figure 6 is plotted on semi-logarithmic form, the effective roughness height z_o indicated by the zero velocity intercept of the best fit line is approximately 0.02 cm, equivalent to a field value of 4 cm, and is reasonable for flat terrain. The turbulence intensity profile is also characteristic of a flat terrain area.

3.2 Experimental Measurements of Mean Velocity in the Wake of the EOCR Complex

Detailed wake measurements for a single wind direction, viz., one face of the EOCR reactor building perpendicular to the flow (approach wind azimuth = 135°), were obtained, rather than a series of less-detailed measurements at many wind directions. This provided an optimum set of data to compare with the momentum theory.

Figures 7 through 10 show the vertical profiles of mean velocity defect, Delta U, for y/H equals 0.0, +0.33, -0.33 and -0.67, respectively. The profiles were taken from x/H equal 3.0 to 35.0 downwind for various z/H locations. Measurements were made with and without the model EOCR complex at all locations. The maximum vertical extent of the velocity defect wake is 1.4 to 1.8 H near the complex and about 2 to 2.4 H in the far wake region. This is of the same order of magnitude as reported by Woo, Peterka and Cermak (1976) and Kothari, Peterka and Meroney (1979a). The velocity defect decays faster in the positive y/H direction than in the negative y/H direction. This is probably due to the silo and tank building upwind in the negative y/H direction. Flow visualization studies by Woo, Peterka, and Cermak (1976) have shown that the separated region extends to about 3 H downstream of the building. Measurements with a hot-film anemometer are not strictly suitable within this recirculating region. Thus, the results at x/H equal to 3 should only be used as qualitative information.

An interesting feature of the wake is that it extends much farther than those reported by Counihan (1971), Colmer (1971), Lemberg (1973) and Castro and Robins (1975). However, the extent of the wake does agree with the results of Hansen, Peterka and Cermak (1975), Woo, Peterka and Cermak (1976) and Kothari, Peterka and Meroney (1979a).

Such long wake regions are apparently associated with the low roughness which characterizes the EOCR site.

Examinations of Figures 7 through 10 also show that none of these decay curves go negative before asymptoting to zero. Similar findings were reported by Woo, Peterka and Cermak (1976). The negative values of Delta U observed by Kothari, Peterka, and Meroney (1979a) was the result of the trailing horseshoe vortices. Hence it might be concluded that the complex EOCR building geometry destroys these vortices so that their effect is very small. Flow visualizations by Hatcher et al. (1977) confirm this; hence, only momentum wake theory has been compared to the present data set.

The maximum velocity defects occurring at each x/H for various y/H positions are shown in Figure 11. The maximum velocity defect did not occur at the same z/H for each x/H value.

3.3 Comparison of the Experimental Measurements of Mean Velocity with the Theory

The theory of wakes behind buildings deeply immersed in a turbulent boundary layer was discussed in Chapter I. This theory is evaluated in this section. Since the theory contains the basic physical mechanism, it should predict a wake reasonably well. The theoretical assumptions that power-law exponent $n << 1$, and $H/\delta << 1$ are satisfied for the present measurements.

In order to compare velocity defect data to the wake theory, the force coefficient for the EOCR complex is required. This was determined by measuring pressures on the building faces. Three hundred and fifteen pressure taps were made on the various faces of building complex, and mean and fluctuating pressures were recorded using the method described

in Chapter II. The forces on the buildings were obtained by assigning an appropriate area to each pressure tap and vector summing the products of pressure times its representative area. The forces on the buildings were then expressed by force coefficients:

$$C_{Fx} = F_x/(0.5\ \rho\ \bar{U}_A^2 A_x)\ ,$$

$$C_{Fy} = F_y/(0.5\ \rho\ \bar{U}_A^2 A_y)\ ,\ \text{and} \qquad [3.2]$$

$$C_{Fz} = F_z/(0.5\ \rho\ \bar{U}_A^2 A_z)\ ,$$

where A_x, A_y and A_z are projected building areas and F_x, F_y and F_z are the resultant forces in x, y and z directions respectively, ρ is the air density and $\bar{U}_A$ is defined as

$$\bar{U}_A = \frac{1}{H}\int_0^H \bar{U}(z)dz\ . \qquad [3.3]$$

Akins, Peterka, and Cermak (1977) have found that the form of $\bar{U}_A$ expressed by Equation (3.3) provides a good collapse of force and moment coefficients for flat-roofed, rectangular buildings of varying aspect ratios. For each building in the EOCR complex, three values of the force coefficients were calculated using its projected area. For the main reactor building the calculated values for C_{Fx}, C_{Fy} and C_{Fz} were 1.09, 0.97 and 0.33, respectively. These values are somewhat smaller than those found by Akins and Cermak (1977) but are probably a result of the different shape of the present structure.

Kothari, Peterka and Meroney (1979a) found that γ and λ equal to one in the wake theory gives good agreement with the velocity defect data. Hence, in the present wake calculation of the constants γ and λ were assumed equal to one. The virtual origin, a, for the wake was

determined from the variation of the experimental data along the assumed wake centerline following a method proposed by Hunt (1971), as shown in Figure 12. The data in this figure unfortunately are not very linear. Castro and Robins (1975) also found that their wind-tunnel results did not follow a straight line. Nonetheless, the data have been approximated by a straight line, and the virtual origin for the wake was estimated to be -2.0 H. The theoretical predictions are not highly sensitive to this value. The prediction of mean velocity defect suggested by the momentum wake theory was then calculated using Equation [1.2]. The vertical profiles of calculated mean velocity defect, Delta U, due to the momentum wake for various x/H locations for y/H equal to 0.0, +0.33, -0.33 and -0.67 are also shown by a dotted line in Figures 7 through 10 respectively. The comparison between the data and wake theory for mean velocity defect is satisfactory, except for the case of y/H equal to -0.67. The comparison also deteriorates in the near wake region, as expected, since this region cannot be considered as a small perturbation to the approach flow. The apparent effect of the wake of silo and tank buildings is evident in the wake data at y/H = -0.67, with higher measured Delta U than predicted by theory.

The maximum Delta U observed and calculated at each x/H location for various y/H positions is shown in Figure 11. The maximum Delta U measurement compares well with the theoretical prediction of momentum wake theory except at y/H equal to -0.67. Thus, it could be concluded that the wake theory predicts the velocity defect satisfactorily along and near the centerline of the principal building in the complex. Very far off the centerline of the main building in the complex, the theory underpredicts the velocity defect due to the presence of the additional buildings.

3.4 Experimental Measurements of Turbulence Intensity Variance in the Wake of the EOCR Complex

Extensive measurements of fluctuating velocity in the wake of the EOCR complex were also performed. The vertical profiles of longitudinal turbulence variance excess, Delta Var, in the wake of the EOCR complex for y/H equal to 0.0, +0.33, -0.33 and -0.67 are shown in Figures 13 through 16, respectively. The mean square values of turbulent velocity fluctuation return to an undisturbed state at a faster rate than the mean velocity defect. Similar findings were reported by Peterka and Cermak (1975), Hansen, Peterka, and Cermak (1975), Woo, Peterka, and Cermak (1976) and Kothari, Peterka, and Meroney (1979a). However, the negative value of turbulence variance excess observed by Kothari, Peterka, and Meroney (1979a) was not observed in the present experiment. The latter authors concluded that this effect was due to the trailing horseshoe vortices, not present in this experiment, which brought low turbulence intensity fluid from the top of the turbulent boundary layer along the wake centerline, reducing the turbulence intensity on the wake centerline. The maximum vertical extent of the turbulent wake was about 1.0 to 1.5 H for all y/H locations. Also, the turbulence variance excess was approximately constant from the lowest z/H measured to a height of approximately z/H equal to 1.0 beyond x/H equal to 10. The Delta Var also approaches zero at z/H = 2.0 for all y/H locations.

The maximum Delta Var occurring at each x/H is plotted in Figure 17 for y/H equal to 0.0, +0.33, -0.33 and -0.67. Similar to the behavior of the maximum Delta U, this maximum did not occur at the same z/H at different values of x/H. The wake theory of Hunt (1971) would have predicted a decay rate of -2.0, shown in Figure 17 for comparison with

the data. It can be concluded that the decay rates of turbulence intensity excess variance for all y/H locations show a decay rate very close to -2.0; the theory is in good agreement with the experimental measurements in this regard.

3.5 Comparison of the Experimental Measurements of Turbulent Diffusion with the Theory

Ground-level measurements of concentration distribution were performed by Hatcher et al. (1977) downwind of the model EOCR complex for eight wind directions, three stabilities, and three release heights. The experimental results were discussed in detail by them. Their experimental measurements of ground-level concentration for 135° wind direction and neutral stability are plotted in Figure 18. The theoretical prediction of Korhari, Peterka, and Meroney (1979b) using Equation [1.5] are also shown in the Figure 19. The constant k_3 in Equation [1.5] was evaluated utilizing experimental data at x/H equal to 8.27 and 16.19 for release heights of 22.6 m and 29.0 m, respectively. The comparison between measurements and the analytical prediction is very good for x/H between 5 and 35.

Chapter IV

CONCLUSIONS

The mean velocity, turbulence intensity, and turbulent diffusion behind the EOCR complex deeply submerged in a neutral turbulent boundary layer have been investigated using wind-tunnel tests and mathematical analysis.

The main effects of a momentum-type wake behind a building complex in a neutral boundary layer are to decrease mean velocity and increase turbulence intensity. The complex site geometry breaks down the usual horseshoe vortices so that they do not play an important role in determining wake characteristics. The decay rate of mean velocity defect was smaller than that of turbulence intensity excess variance. The wake was detected at a distance of $x/H = 35$ at a 5 percent mean velocity defect level (or out to 100 H at the 1 percent level). Such long wake regions are apparently associated with the low surface roughness characteristic of the site.

The present experimental results were compared with the momentum wake theory and found to have satisfactory agreement for vertical profiles of velocity defect for all lateral positions y/H measured, except at y/H equal to -0.67. The maximum velocity defect rates compared very well with the theory again, except at y/H equal to 0.67. Thus, it is concluded that the theory predicts the mean velocity defect satisfactorily close to the wake centerline, but underpredicts away from the centerline because of the complex geometry. The experimental measurements of the decay rate of turbulence excess variance were found to compare very well with that predicted by the wake theory for all y/H locations.

The ground-level concertration distribution downwind of the EOCR complex also compared very well with the analytical prediction.

REFERENCES

Abramowitz, M. and Stegun, I. A., 1968, Handbook of Mathematical Functions, National Bureau of Standards, Applied Mathematics Series 55, Washington, D.C.

Akins, R. E. and Cermak, J. E., 1977, "Wind Pressures on Buildings," Fluid Dynamics and Diffusion Report CER76-77REA-JEC15, Colorado State University, Fort Collins, Colorado.

Akins, R. E., Peterka, J. A., and Cermak, J. E., 1977, "Mean Force and Moment Coefficients for Buildings in Turbulent Boundary Layers," Journal of Industrial Aerodynamics, Vol. 2, pp. 195-209.

Bearman, P. W., 1970, "Corrections for the Effect of Ambient Temperature Drift on Hot-Wire Measurements in Incompressible Flow," DISA Information Bulletin No. 11.

Castro, I. P. and Robins, A. G., 1975, "The Effects of a Thick Incident Boundary Layer on the Flow Around a Small Surface Mounted Cube," Central Electricity Generating Board Report R/M/N795.

Cermak, J. E., 1975, "Applications of Fluid Mechanics to Wind Engineering--A Freeman Scholar Lecture," Journal of Fluids Engineering, Trans. of the ASME, Vol. 97, pp. 9-38.

Cermak, J. E. and Arya, S. P. S., 1970, "Problems of Atmospheric Shear Flows and Their Laboratory Simulations," AGARD Conference Proceedings, No. 48, pp. 12.1-12.16.

Colmer, M. J., 1971, "Some Full-Scale Measurements of the Flow in the Wake of a Hanger," ARC-CP-1166.

Counihan, J., 1971, "An Experimental Investigation of the Wake Behind a Two-Dimensional Block and Behind a Cube in a Simulated Boundary Layer Flow," CERL Lab. Note: RD/L/N115/71.

Frost, W. and Shahabi, A. M., 1977, "A Field Study of Wind Over a Simulated Block Building," NASA Report CR-2804.

Hansen, A. C. and Cermak, J. E., 1975, "Vortex-Containing Wakes of Surface Obstacles," Fluid Dynamics and Diffusion Laboratory Report CER75-76ACH-JEC16, Colorado State University, Fort Collins, Colorado.

Hansen, A. C., Peterka, J. A., and Cermak, J. E., 1975, "Wind-Tunnel Measurements in the Wake of a Simple Structure in a Simulated Atmospheric Flow," Fluid Dynamics and Diffusion Laboratory Report CER73-74ACH-JAP-JEC43, Colorado State University, Fort Collins, Colorado.

Hatcher, R. V., Meroney, R. N., Peterka, J. A., and Kothari, K. M., 1977, 'Dispersion in the Wake of Model Industrial Complex," Fluid Dynamics and Diffusion Laboratory Report CER76-77RVH-RNM-JAP-KMK35, Colorado State University, Fort Collins, Colorado. Also the U.S. Nuclear Regulatory Commission Report NUREG-0373.

Huber, A. H. and Snyder, W. H., 1976, "Building Wake Effects on Short Stack Effluents," Third Symposium on Atmospheric Turbulence Diffusion and Air Quality, October, Raleigh, North Carolina.

Hunt, J. C. R., 1971, "Further Aspects of the Theory of Wakes Behind Buildings and Comparison of Theory with Experiments," Central Electricity Research Laboratory Report RD/L/R/1665.

Hunt, J. C. R., 1975, "Vortex and Momentum Wakes Behind Surface Obstacles in Turbulent Boundary Layers," to be published.

Hunt, J. C. R. and Smith, J. P., 1969, "A Theory of Wakes Behind Buildings and Some Provisional Experimental Results," Central Electricity Research Laboratory Report RD/L/N31/69.

Kothari, K. M., Peterka, J. A., and Meroney, R. N., 1979a, "Stably Stratified Building Wakes," Fluid Dynamics and Diffusion Laboratory Report CER78-79KMK-JAP-RNM65, Colorado State University, Fort Collins, Colorado. Also the U.S. Nuclear Regulatory Commission Report NUREG/CR-1247.

Kothari, K. M., Peterka, J. A., and Meroney, R. N., 1979b, "An Analytical Method for Determination of Dispersion in the Wake of a Power Plant," to be published.

Lemberg, R., 1973, "On the Wakes Behind Bluff Bodies in a Turbulent Boundary Layer," University of Western Ontario Report BLWT-3-73.

Marsh, G. L. and Peterka, J. A., 1977, "Measurements of Turbulent Flows with a Rotated Hot-Film Anemometer," Fluid Dynamics and Diffusion Laboratory Report CER76-77GLM-JAP64, Colorado State University, Fort Collins, Colorado.

Peterka, J. A. and Cermak, J. E., 1975, "Turbulence in Building Wakes," Fourth International Conference on Wind Effects on Buildings and Structures, London, September.

Sandborn, V. A., 1972, Resistance Temperature Transducer, Metrology Press, Fort Collins, Colorado.

Schlichting, H., 1979, Boundary Layer Theory, McGraw-Hill Book Co., New York, N. Y.

Smith, F. B., 1957, "The Diffusion of Smoke from a Continuous Elevated Point-Source into a Turbulent Atmosphere," Journal of Fluid Mechanics, Vol. 2, Part 1, pp. 49-76.

Snyder, W. H., 1972, "Similarity Criteria for the Application of Fluid Models to the Study of Air Pollution Meteorology," Boundary Layer Meteorology, Vol. 3, No. 1, September.

Snyder, W. H., 1981, Guideline for Fluid Modeling of Atmospheric Diffusion, U.S. Environmental Protection Agency Report, EPA 600/8-81-009, 185 pp.

Woo, H. G. C., Peterka, J. A., and Cermak, J. E., 1976, "Wind-Tunnel Measurements in the Wakes of Structures," Fluid Dynamics and Diffusion Laboratory Report CER75-76HGCW-JAP-JEC40, Colorado State University, Fort Collins, Colorado.

Zambrano, T. G. and Peterka, J. A., 1978, "Wind Load Interaction on an Adjacent Building," Fluid Dynamics and Diffusion Laboratory Report CER77-78TGZ-JAP26, Colorado State University, Fort Collins, Colorado.

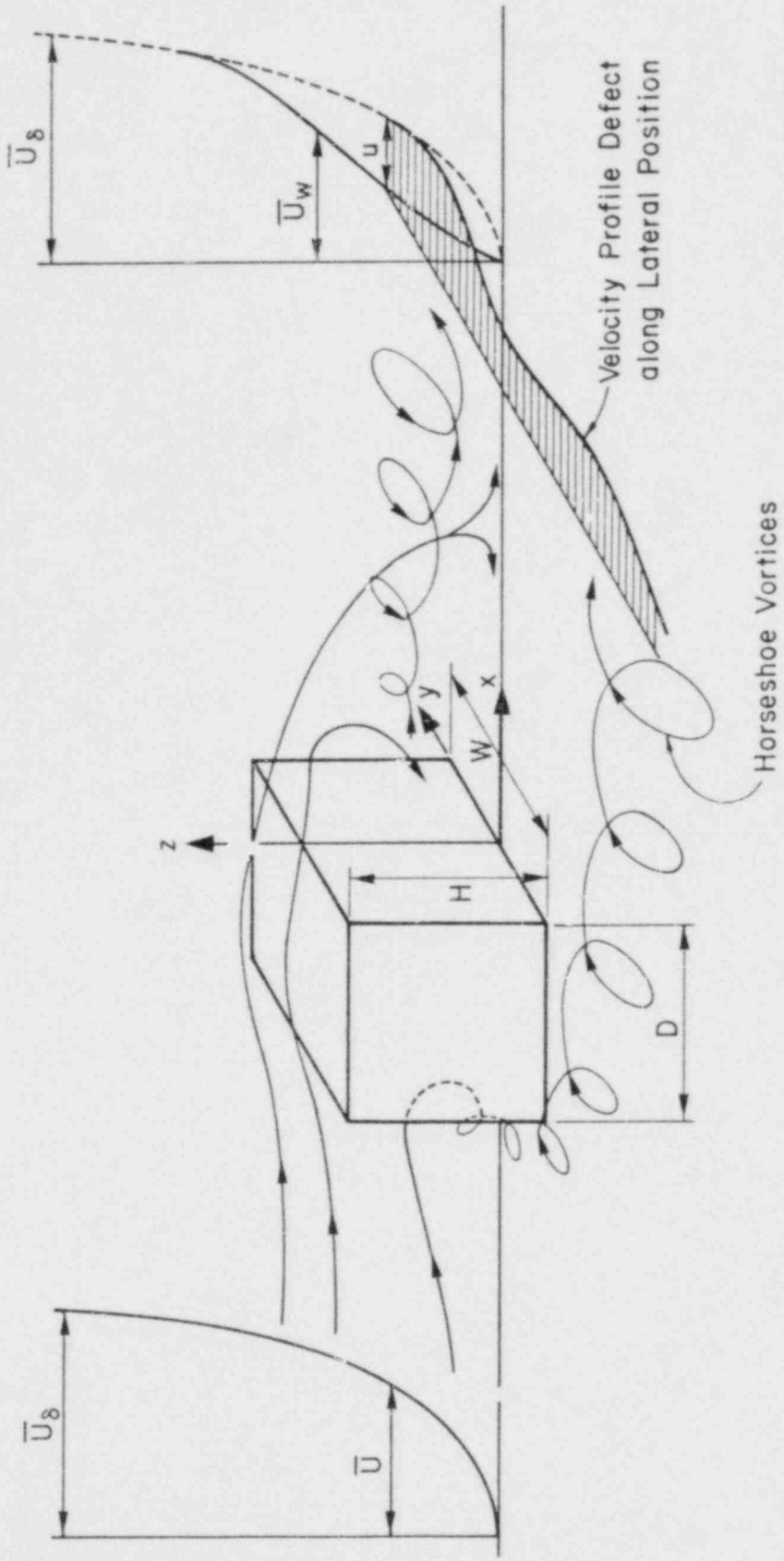

Figure 1. Flow pattern around a rectangular building.

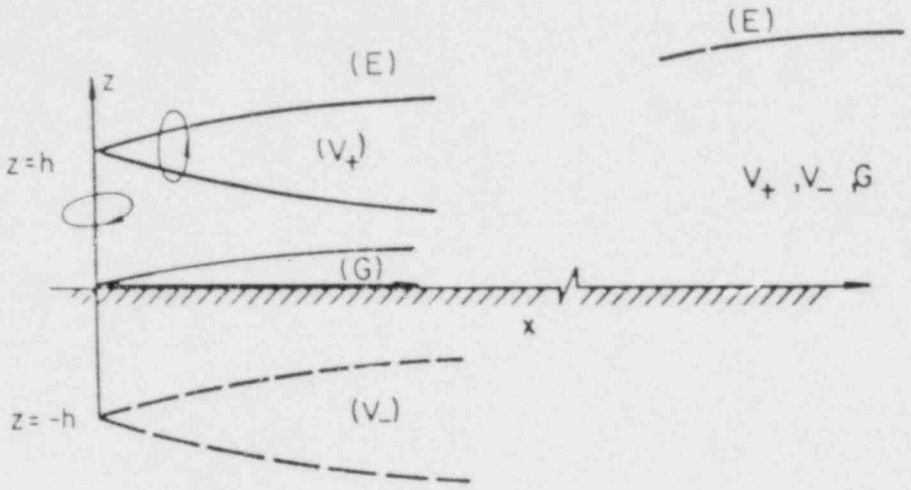

(a) Side View

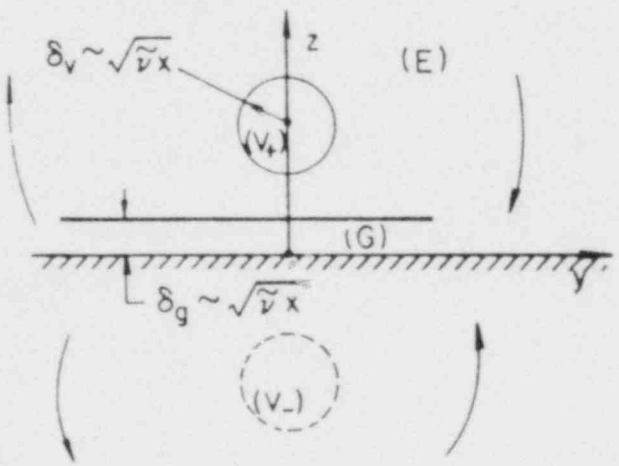

(b) Looking Upwind $h >> \sqrt{\tilde{\nu} x}$

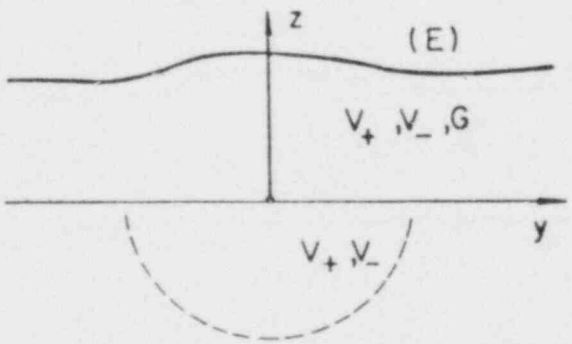

Figure 2. Schematic of the regions of influence of vortex core and the vortex-induced boundary layer (from the vortex wake theory of Hunt, 1975).

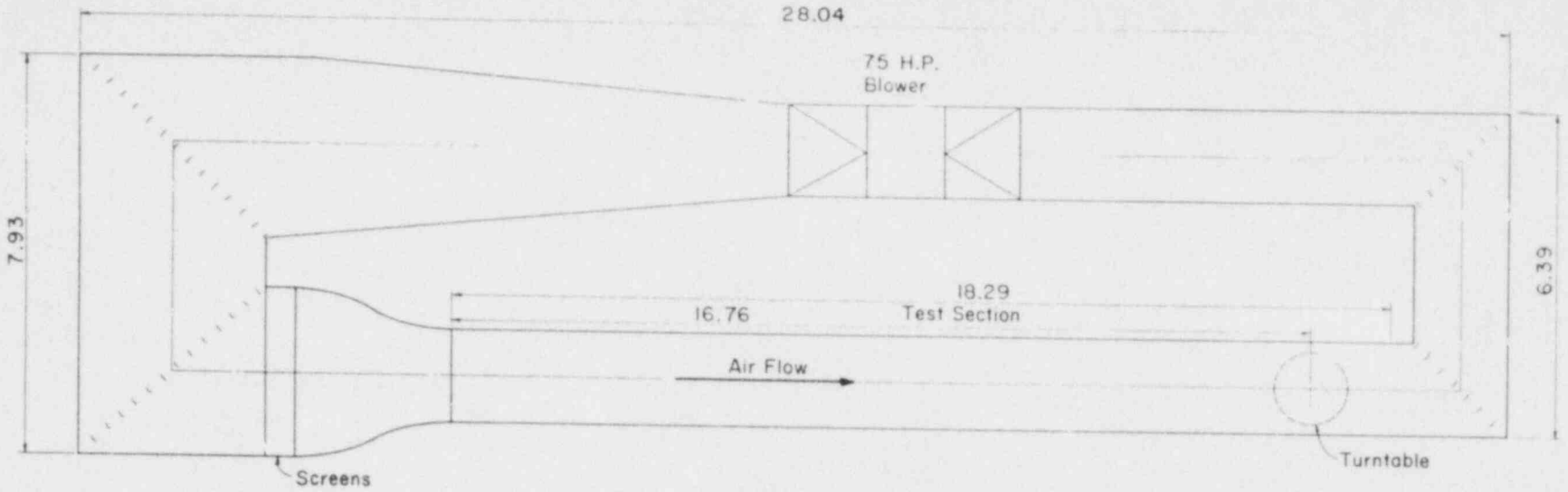

PLAN

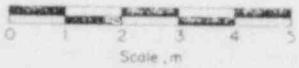

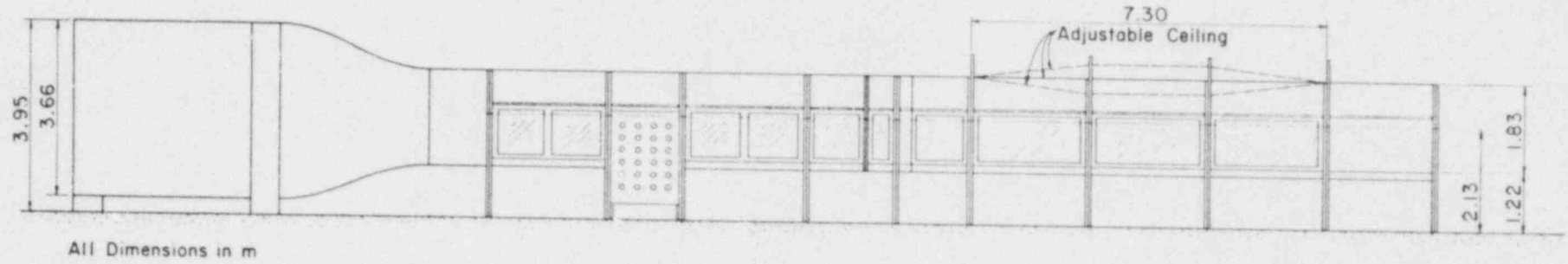

ELEVATION

Figure 3. Industrial Wind Tunnel, Fluid Dynamics and Diffusion Laboratory, Colorado State University.

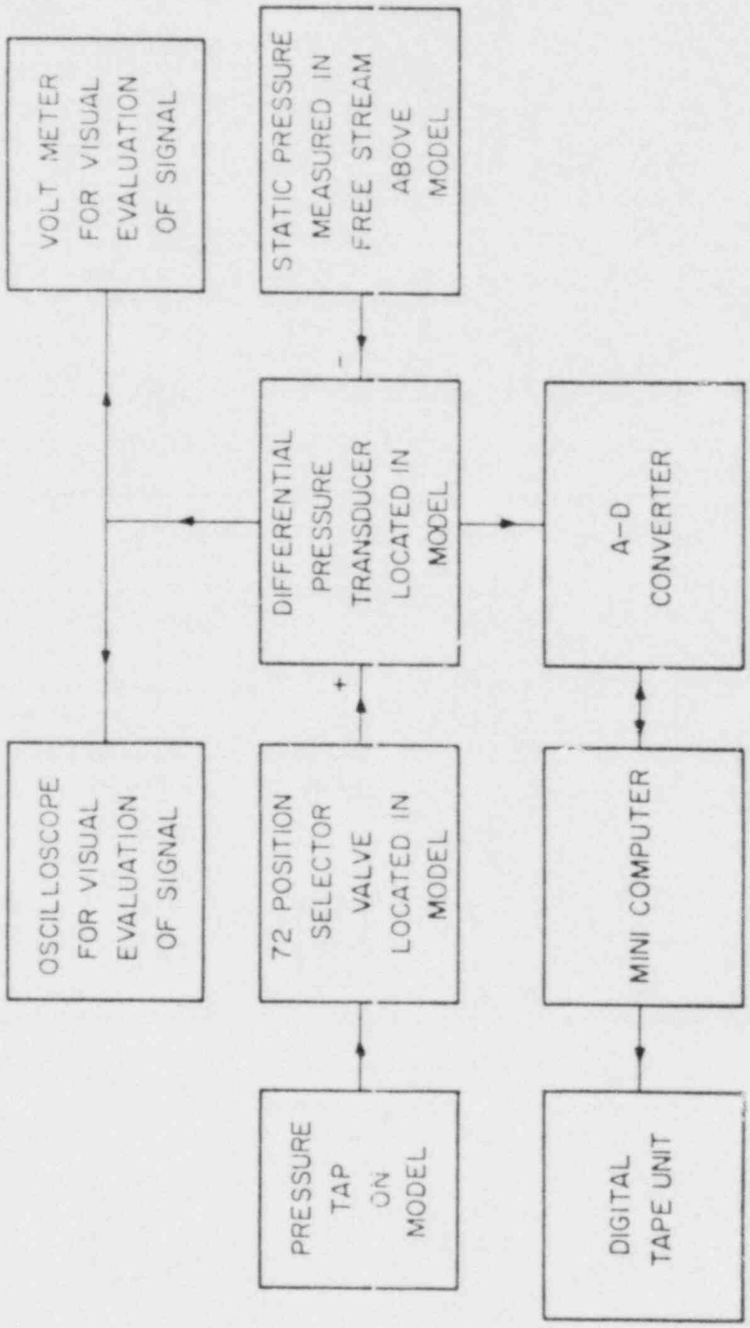

Figure 4. Schematic of data-acquisition system for pressure measurements.

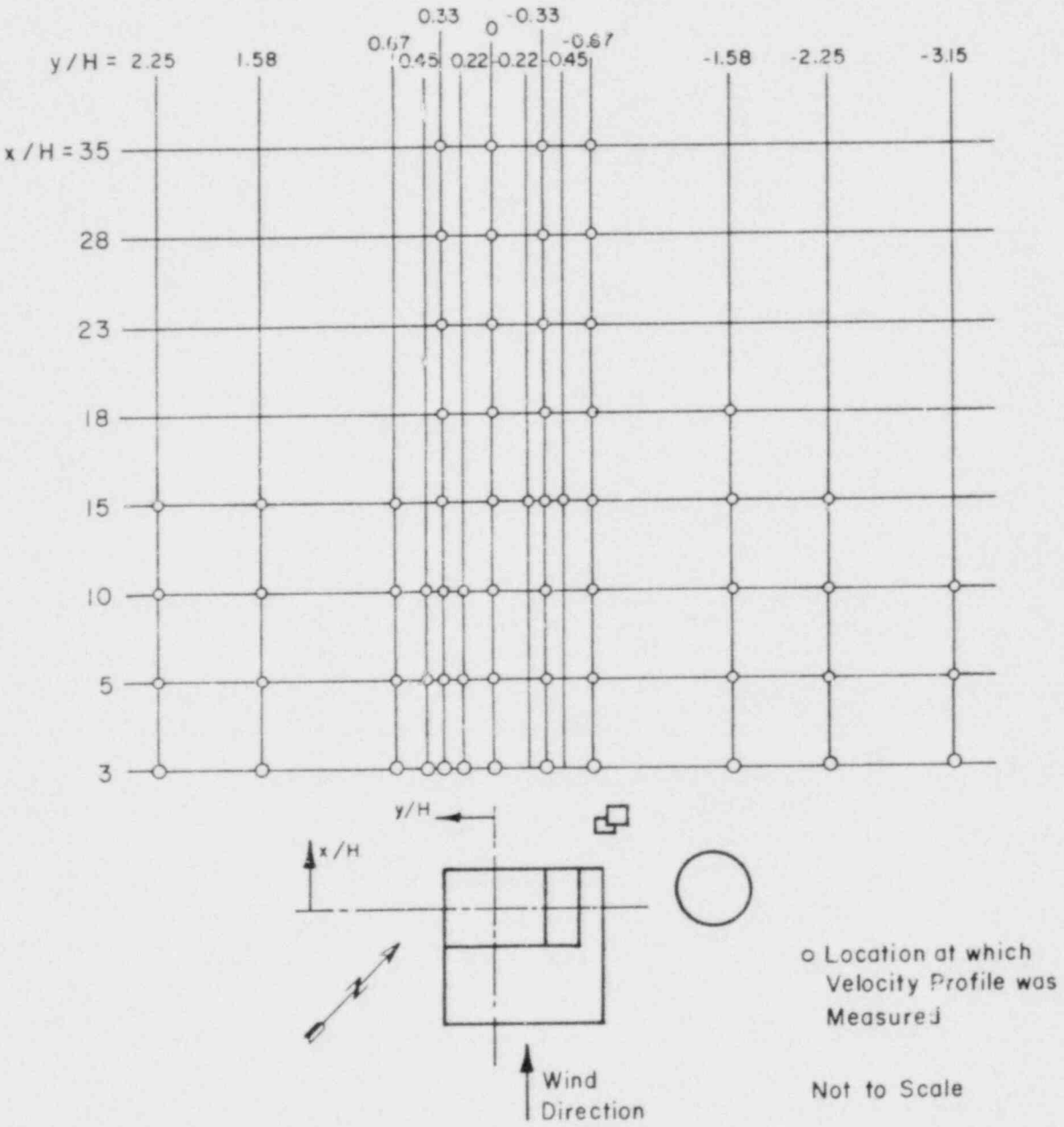

Figure 5. Velocity profiles measurement locations and the EOCR configuration.

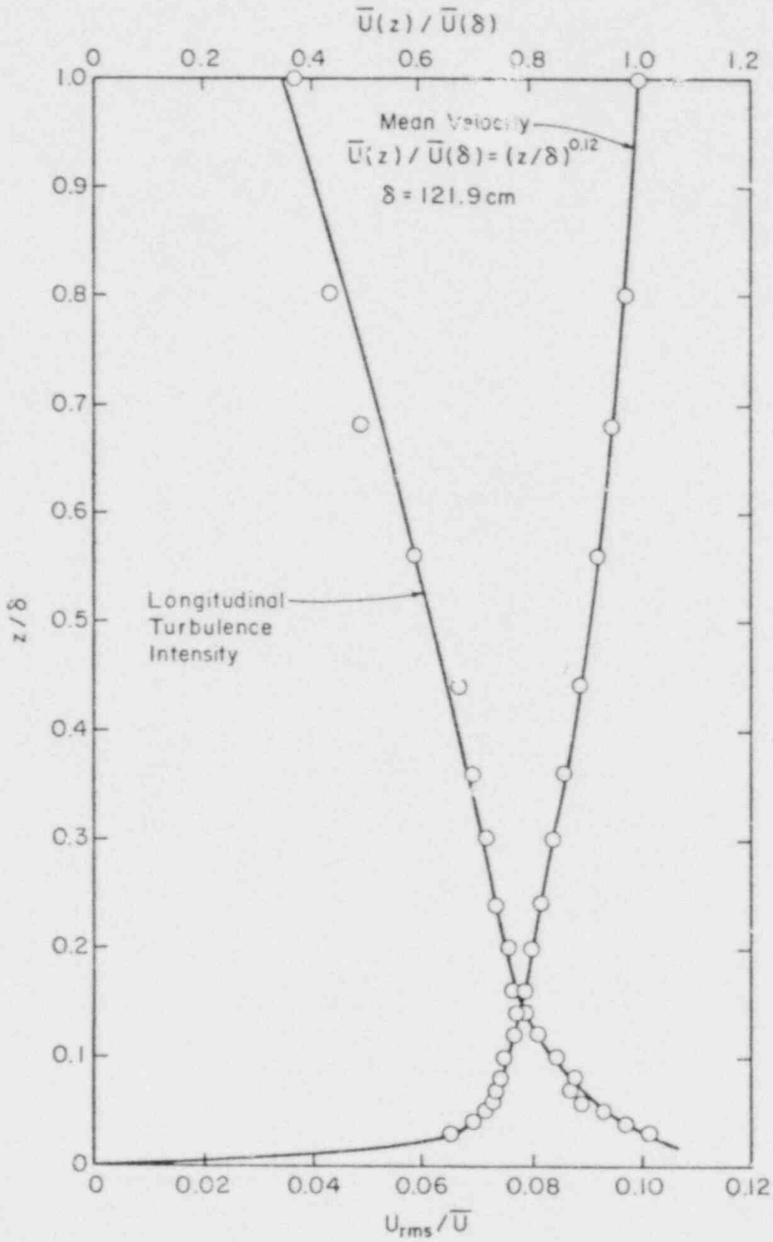

Figure 6. Approach flow characteristics.

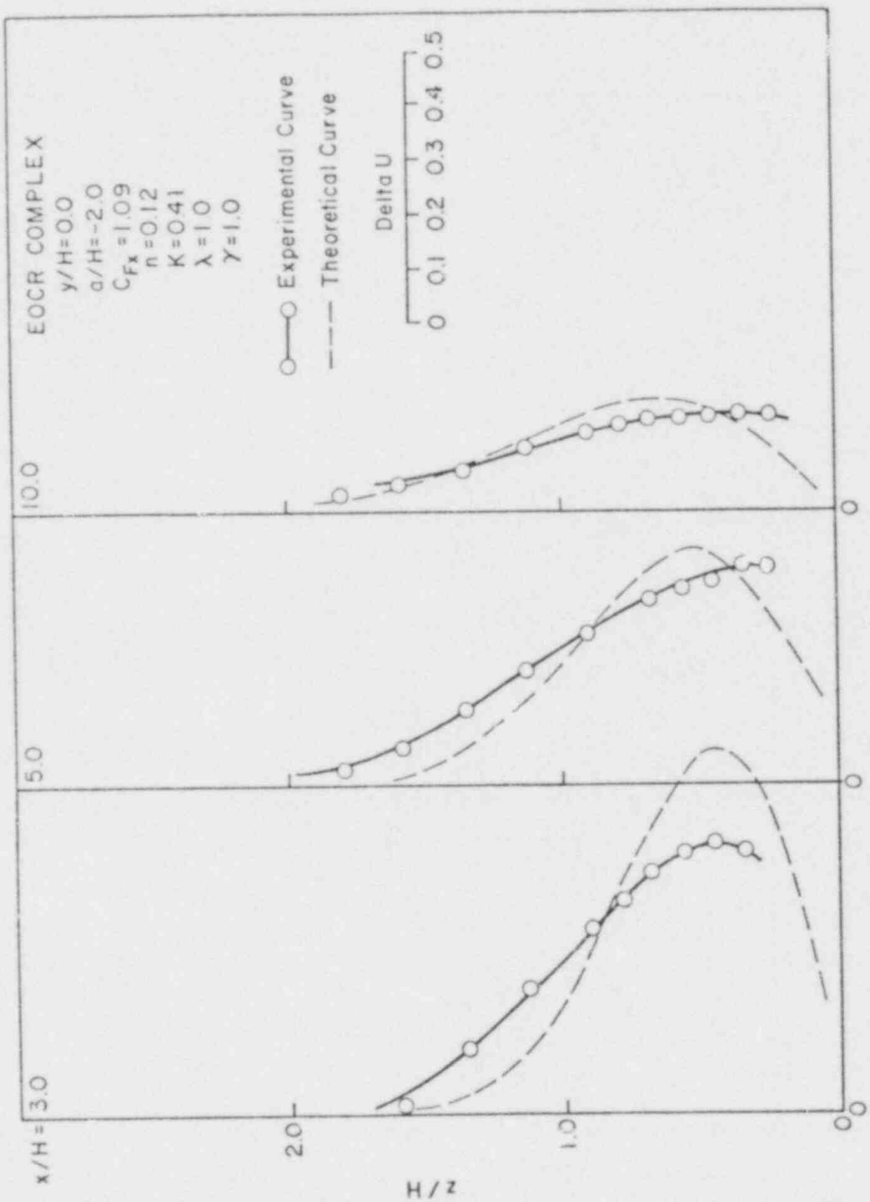

Figure 7a. Comparison of the measured vertical profiles of velocity defect with the momentum wake theory for y/H = 0.0.

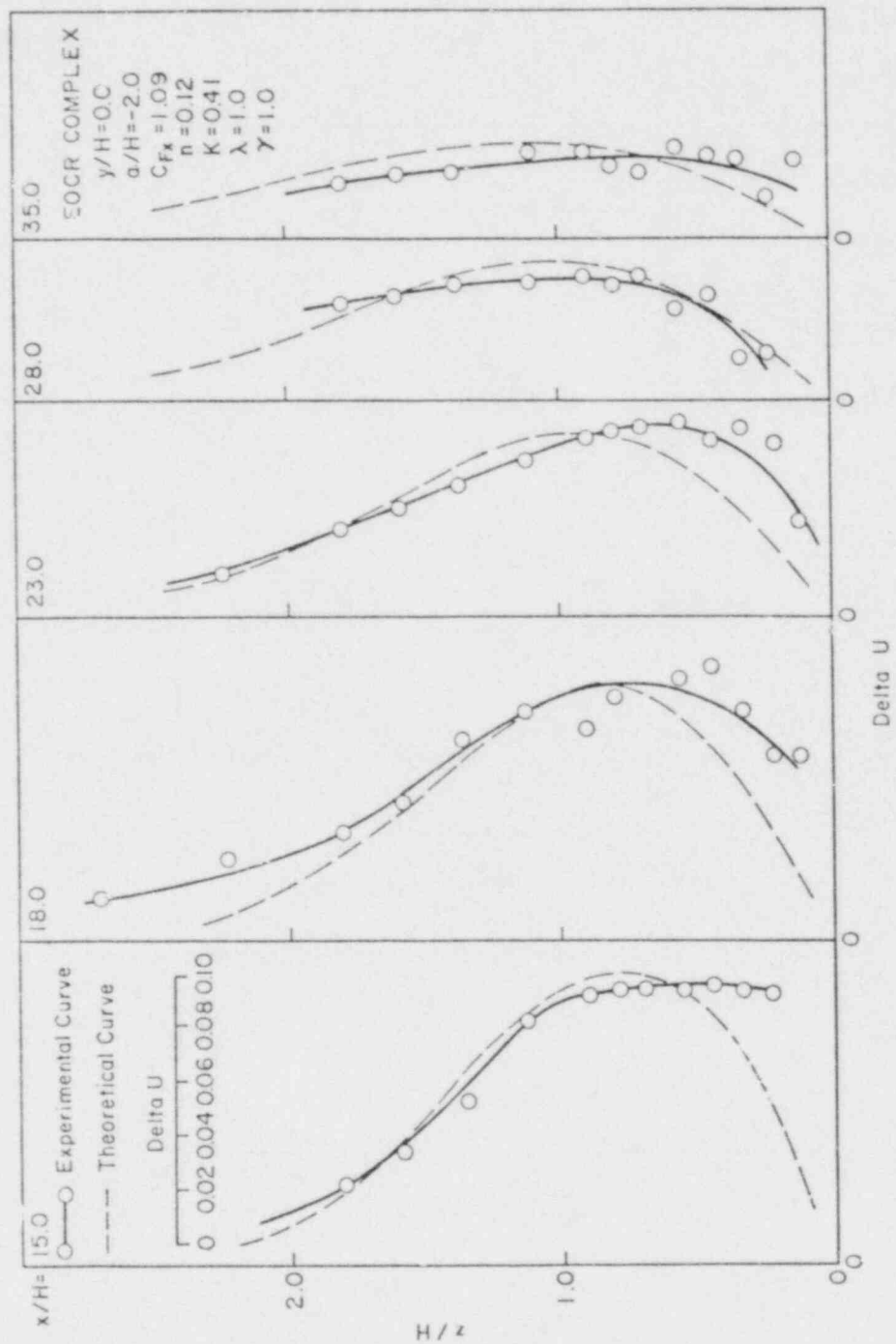

Figure 7b. Comparison of the measured vertical profiles of velocity defect with the momentum wake theory for y/H = 0.0 (continued).

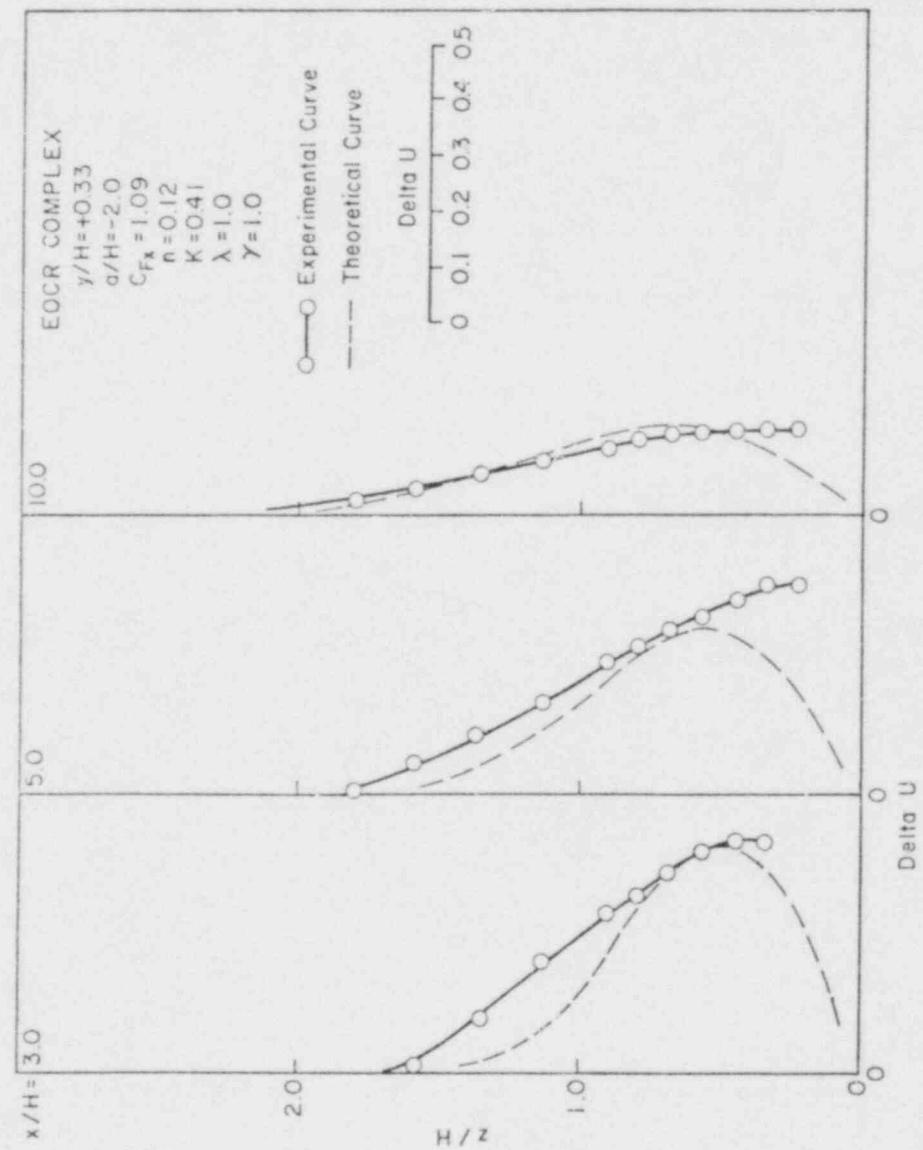

Figure 8a. Comparison of the measured vertical profiles of velocity defect with the momentum wake theory for y/H = 0.33.

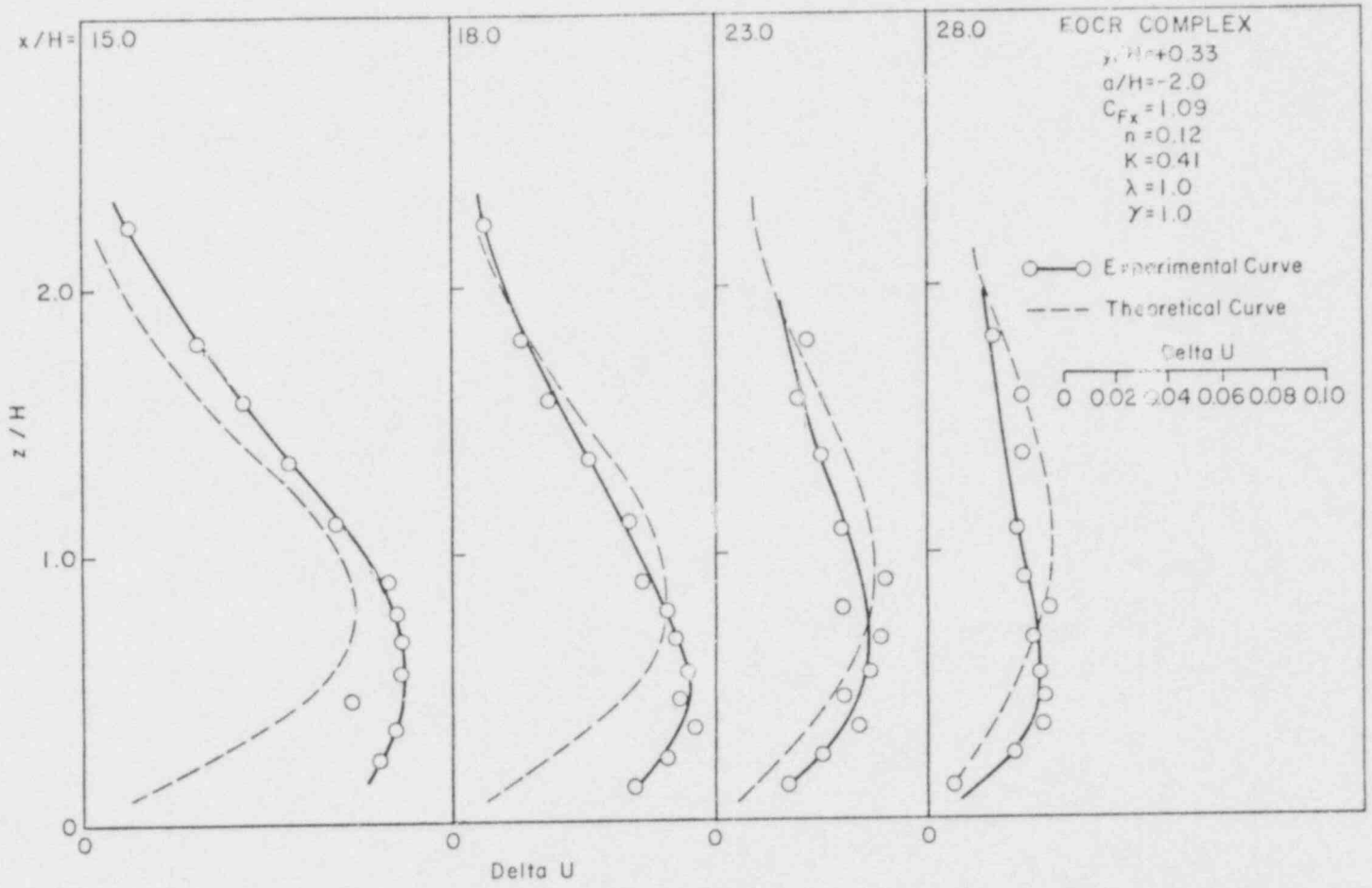

Figure 8b. Comparison of the measured vertical profiles of velocity defect with the momentum wake theory for y/H = 0.33 (continued).

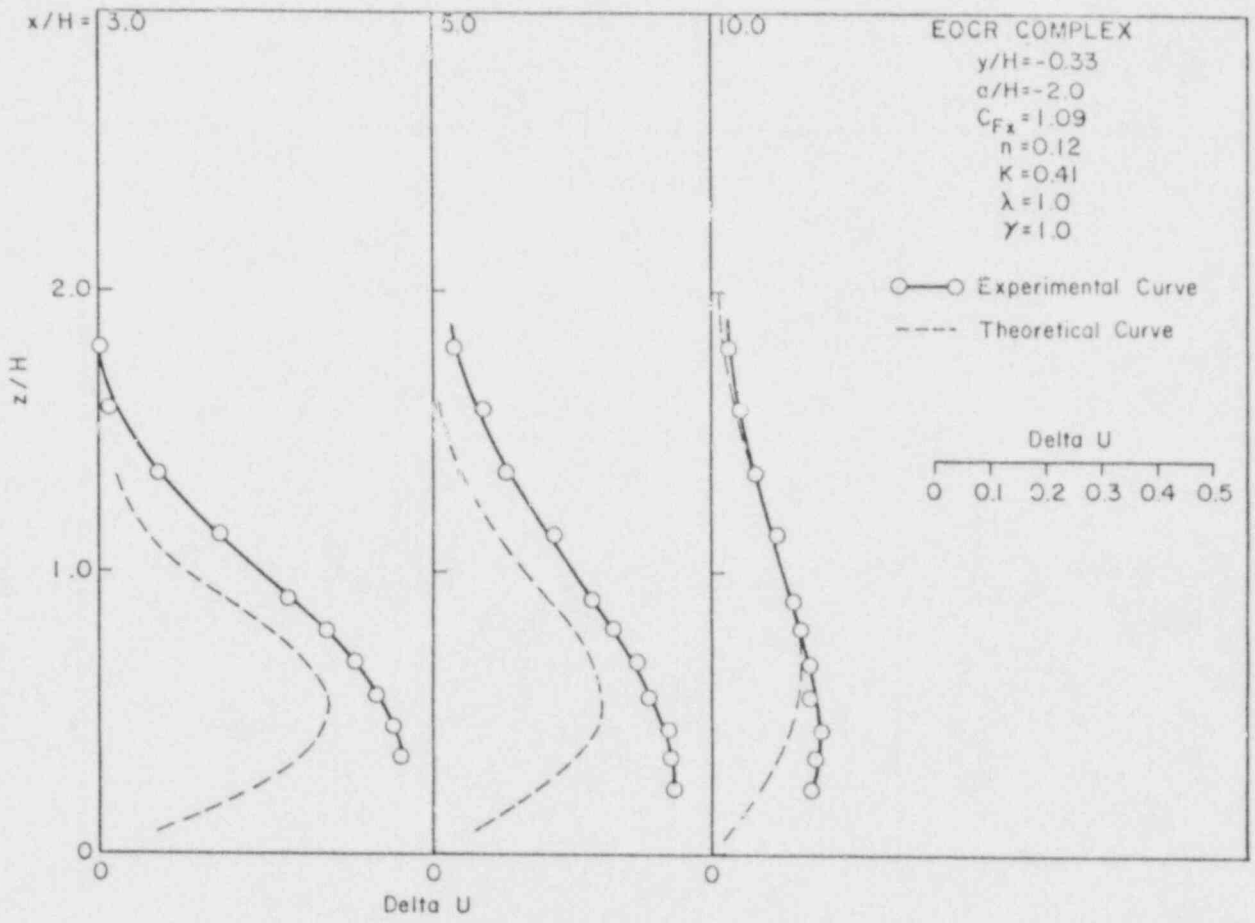

Figure 9a. Comparison of the measured vertical profiles of velocity defect with the momentum wake theory for y/H = -0.33.

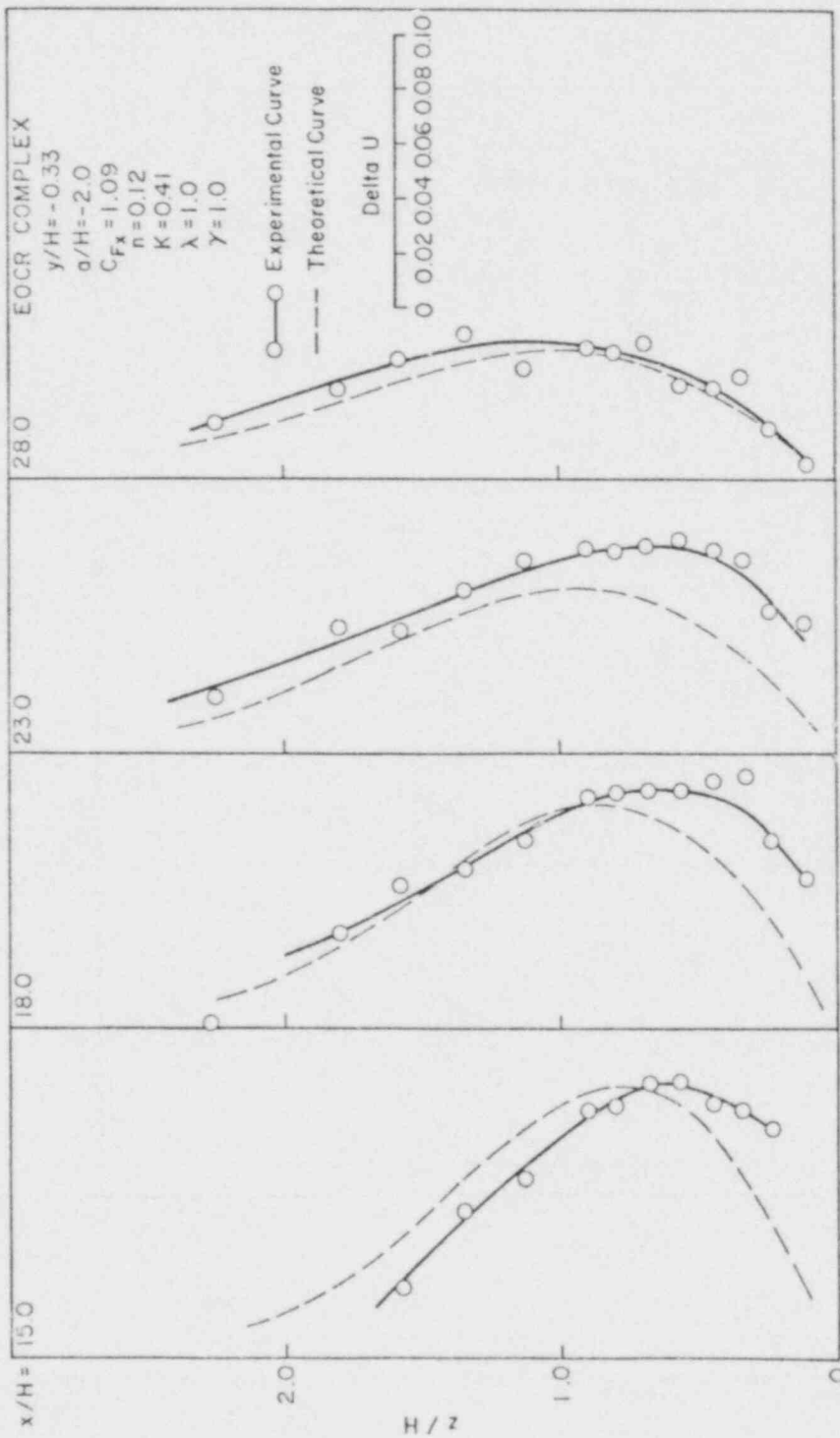

Figure 9b. Comparison of the measured vertical profiles of velocity defect with the momentum wake theory for y/H = -0.33 (continued).

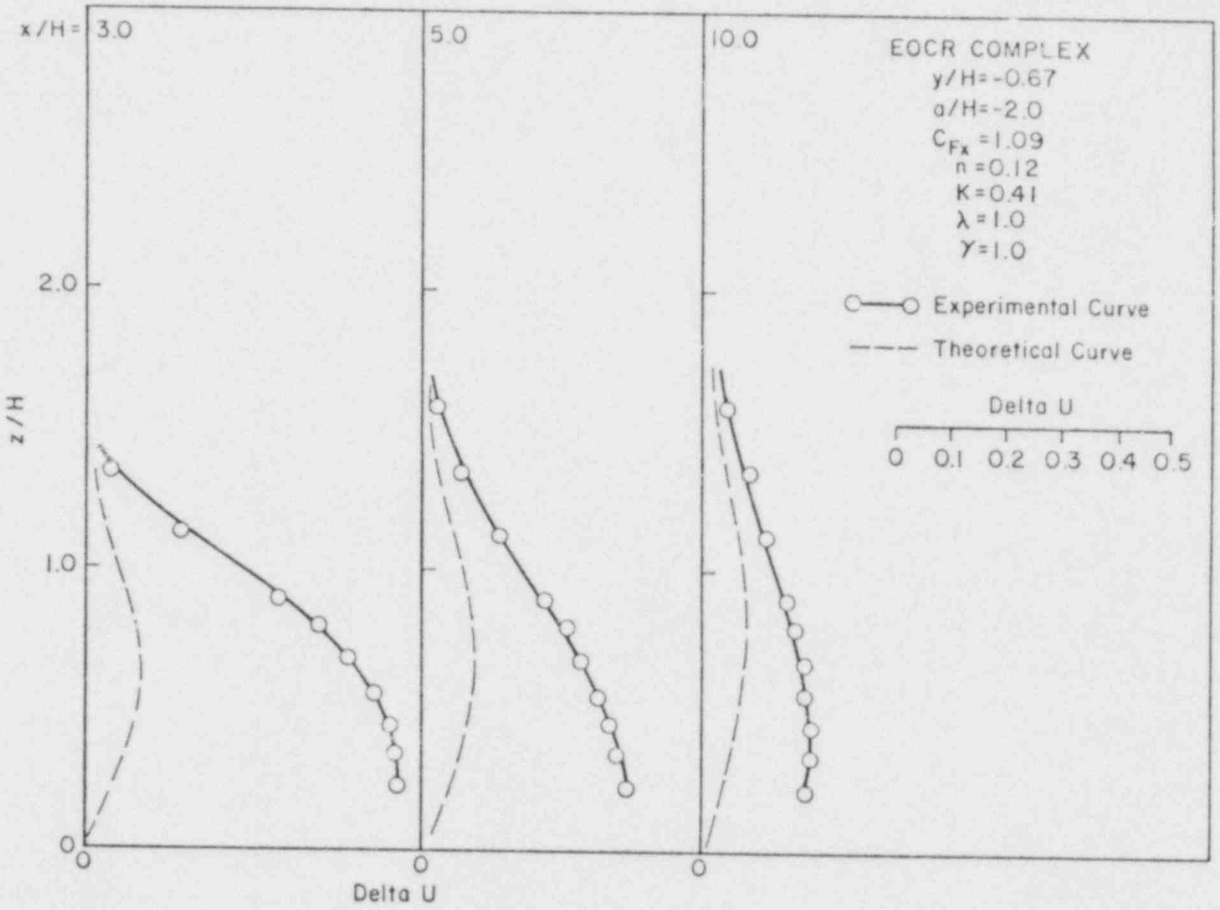

Figure 10a. Comparison of the measured vertical profiles of velocity defect with the momentum wake theory for y/H = -0.67.

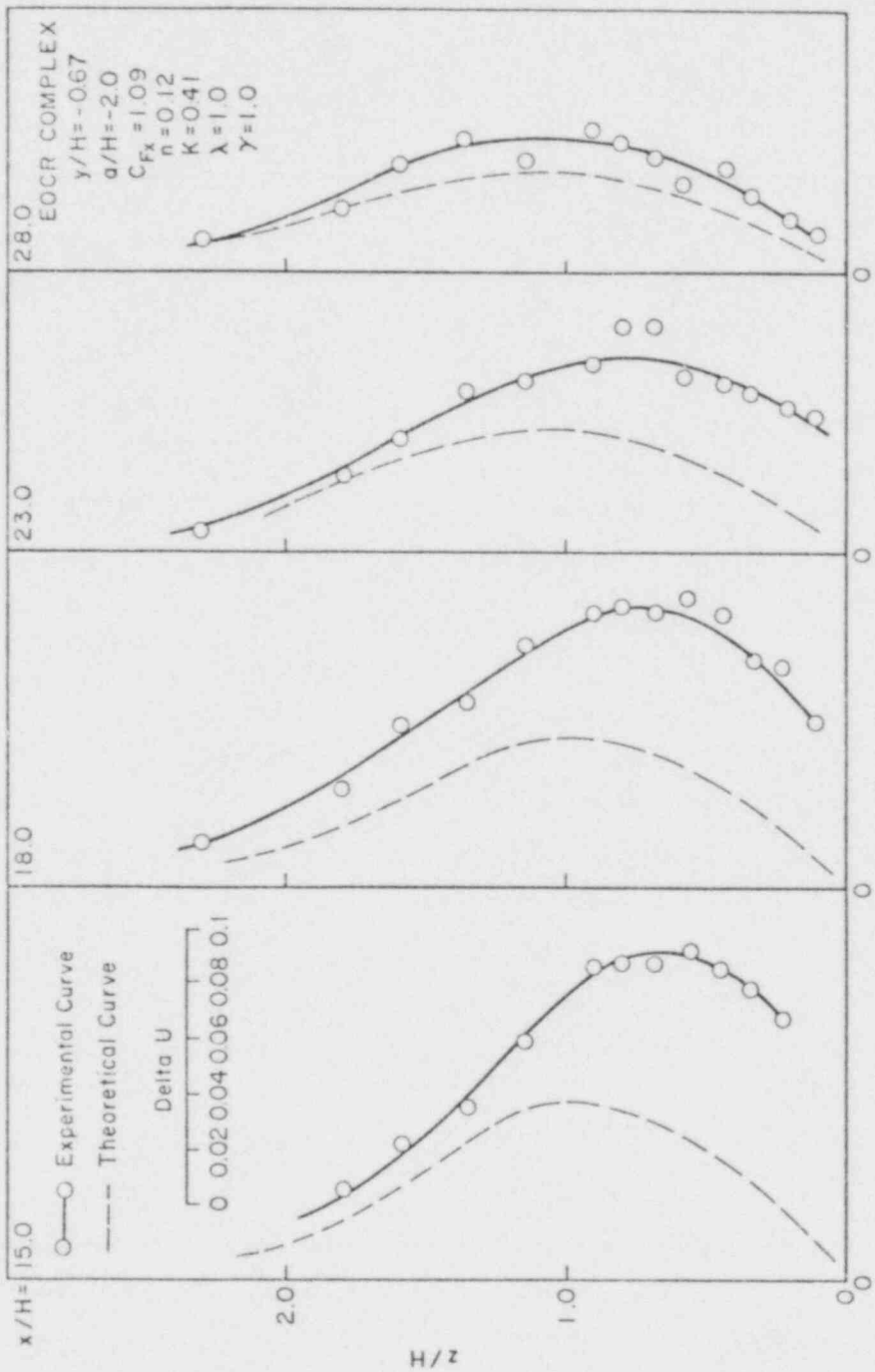

Figure 10b. Comparison of the measured vertical profiles of velocity defect with the momentum wake theory for y/H = -0.67 (continued).

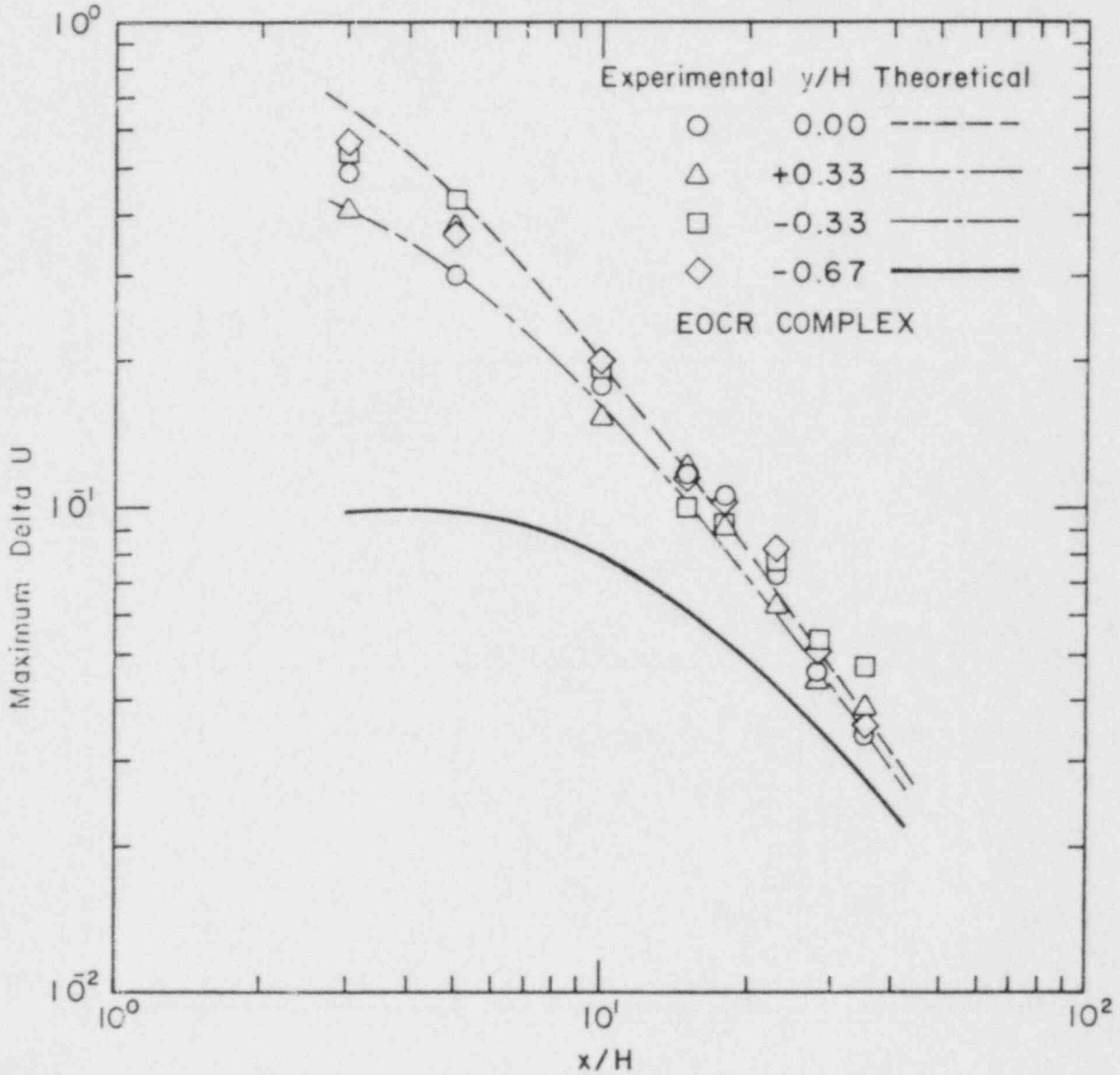

Figure 11. Comparison of the decay rates of mean velocity defect in the wake of the EOCR complex to the momentum wake theory.

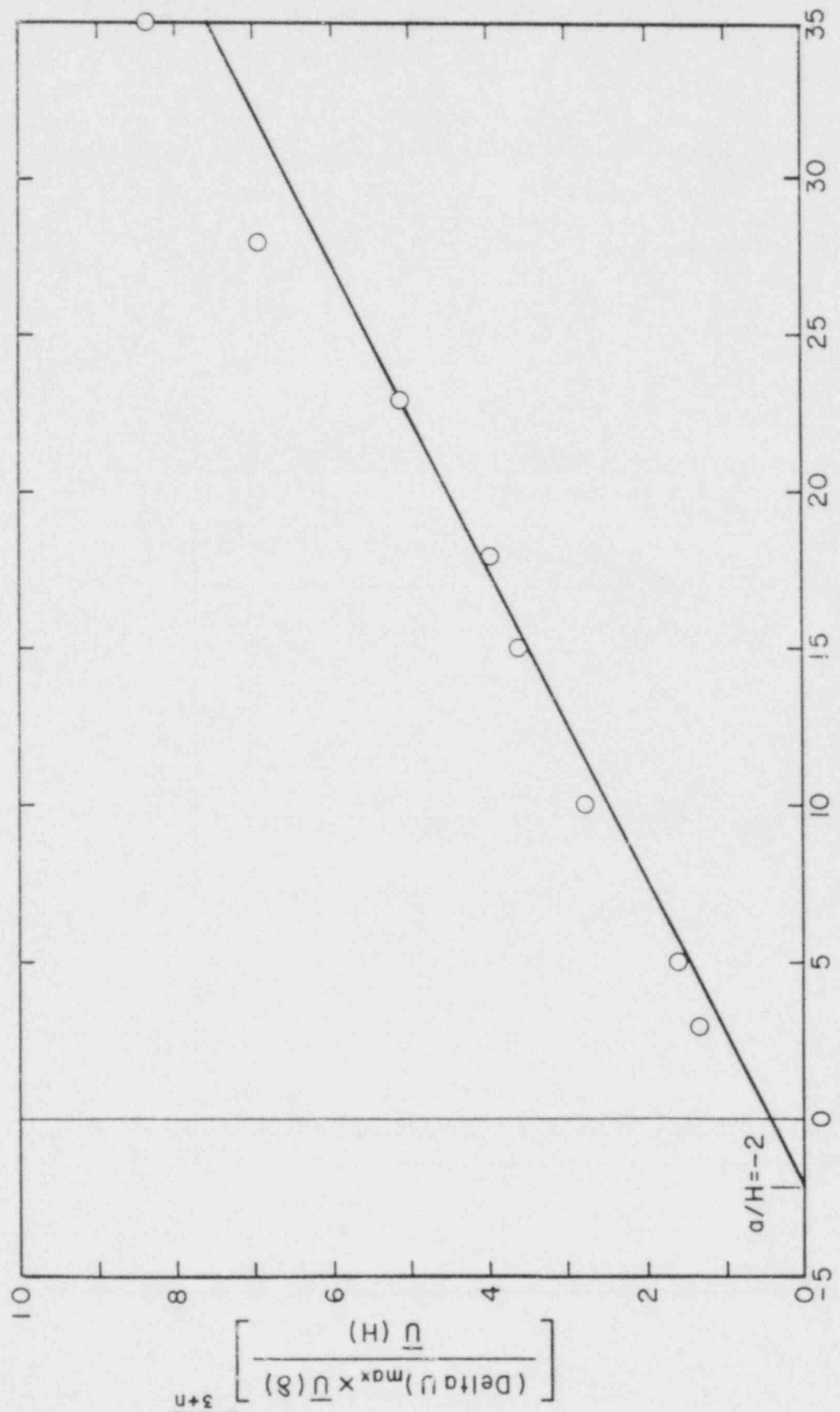

Figure 12. Determination of virtual origin for the EOCR wake.

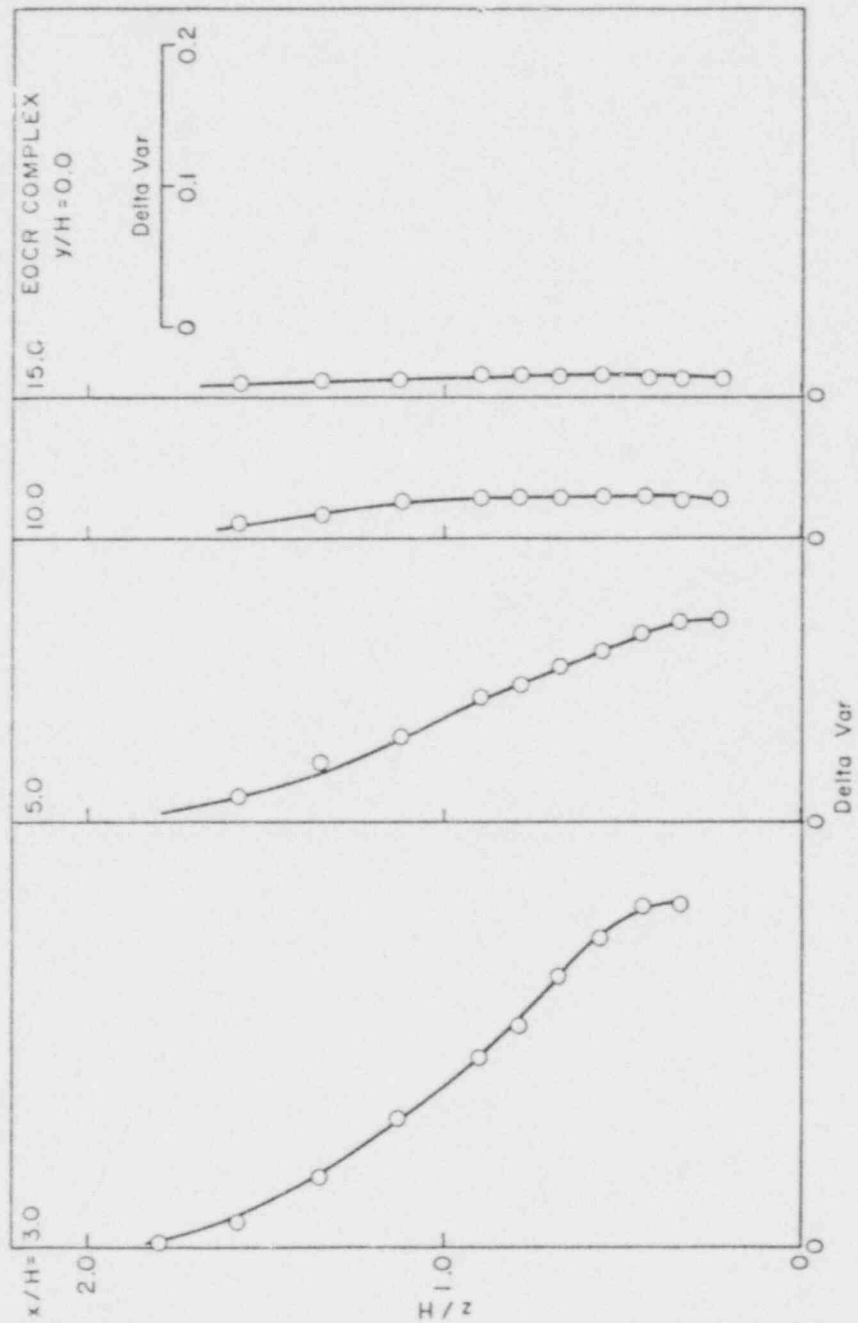

Figure 13. Vertical profiles of turbulence intensity excess variance for y/H = 0.0.

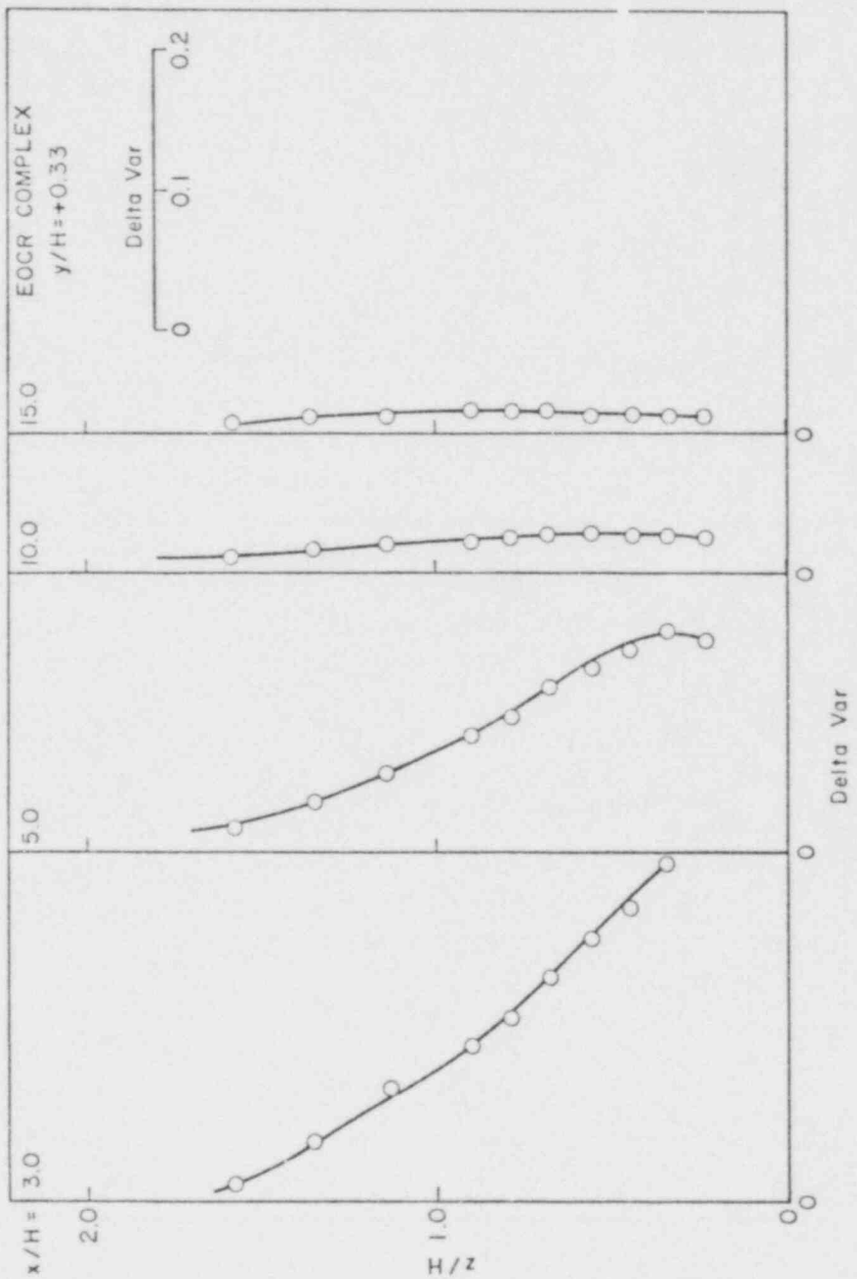

Figure 14. Vertical profiles of turbulence intensity excess variance for y/H = 0.33.

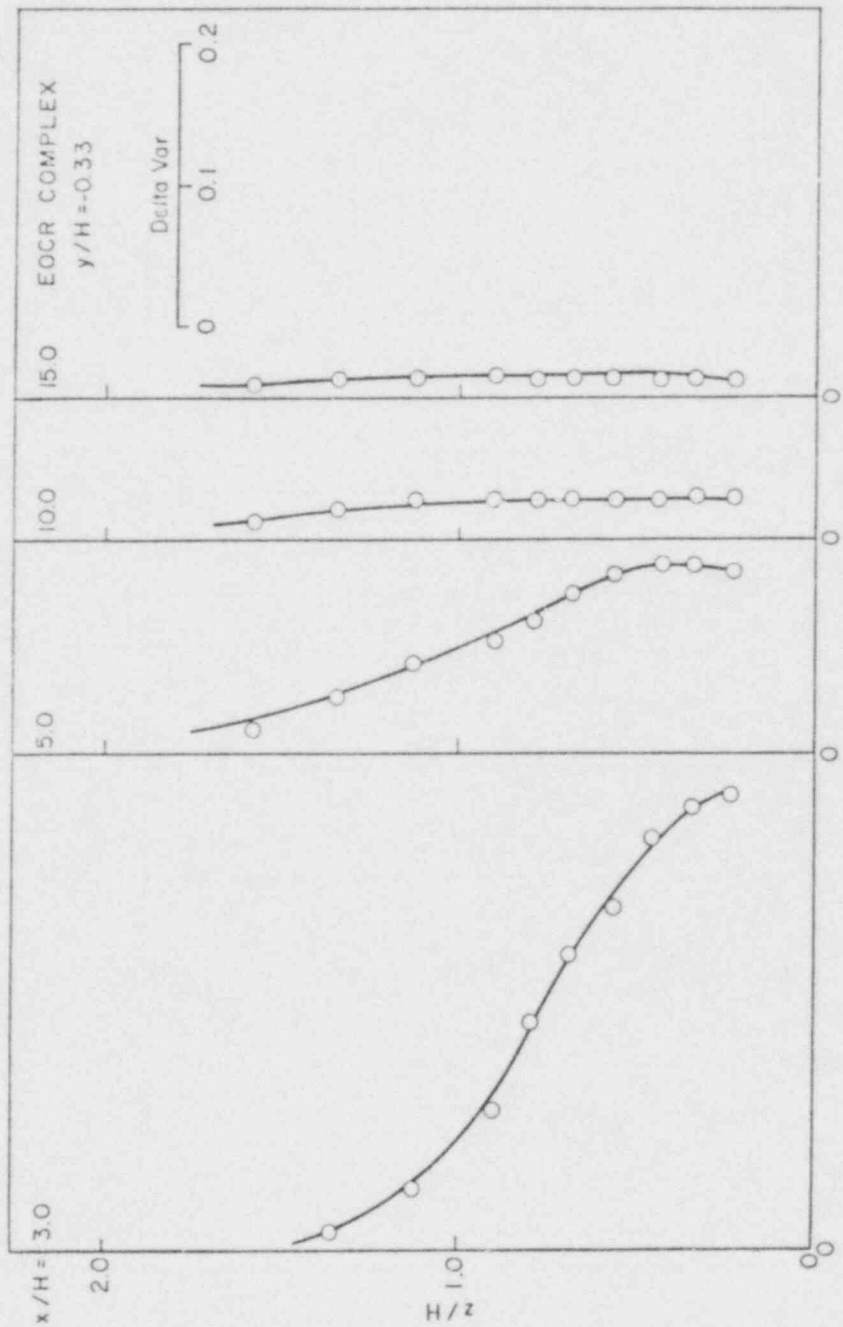

Figure 15. Vertical profiles of turbulence intensity excess variance for y/H = -0.33.

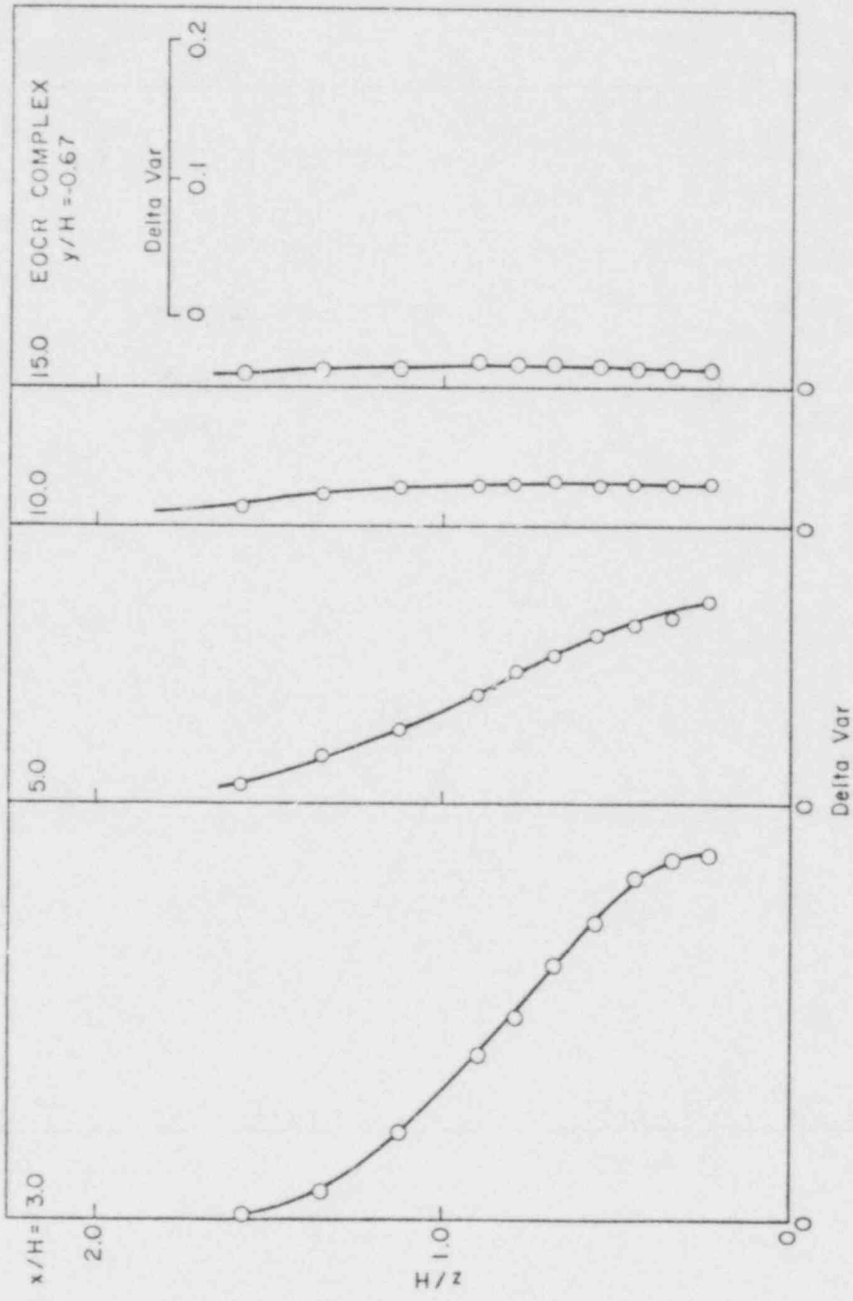

Figure 16. Vertical profiles of turbulence intensity excess variance for y/H = -0.67.

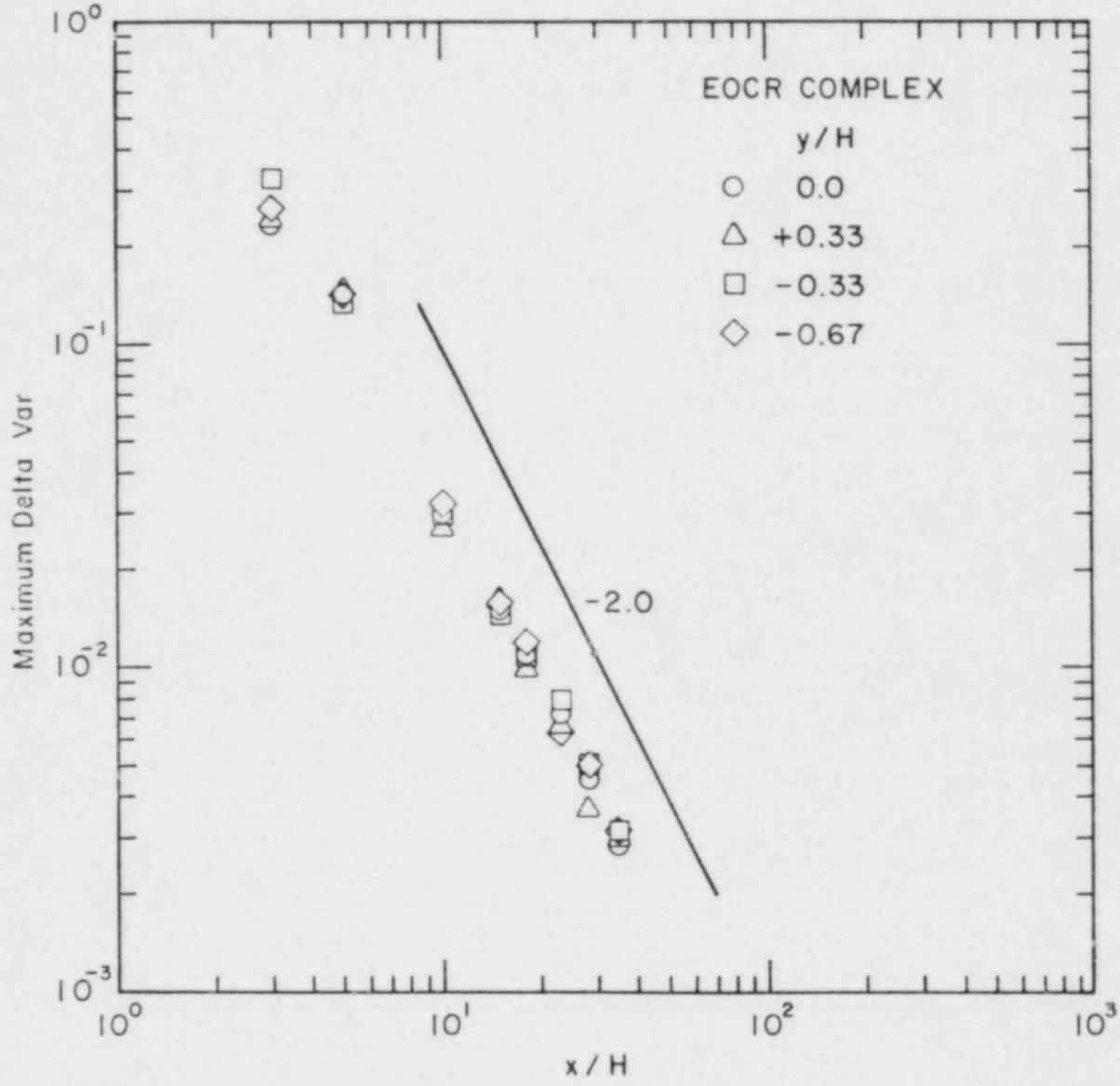

Figure 17. Comparison of the decay rates of turbulence intensity excess variance in the wake of the EOCR complex with the theory.

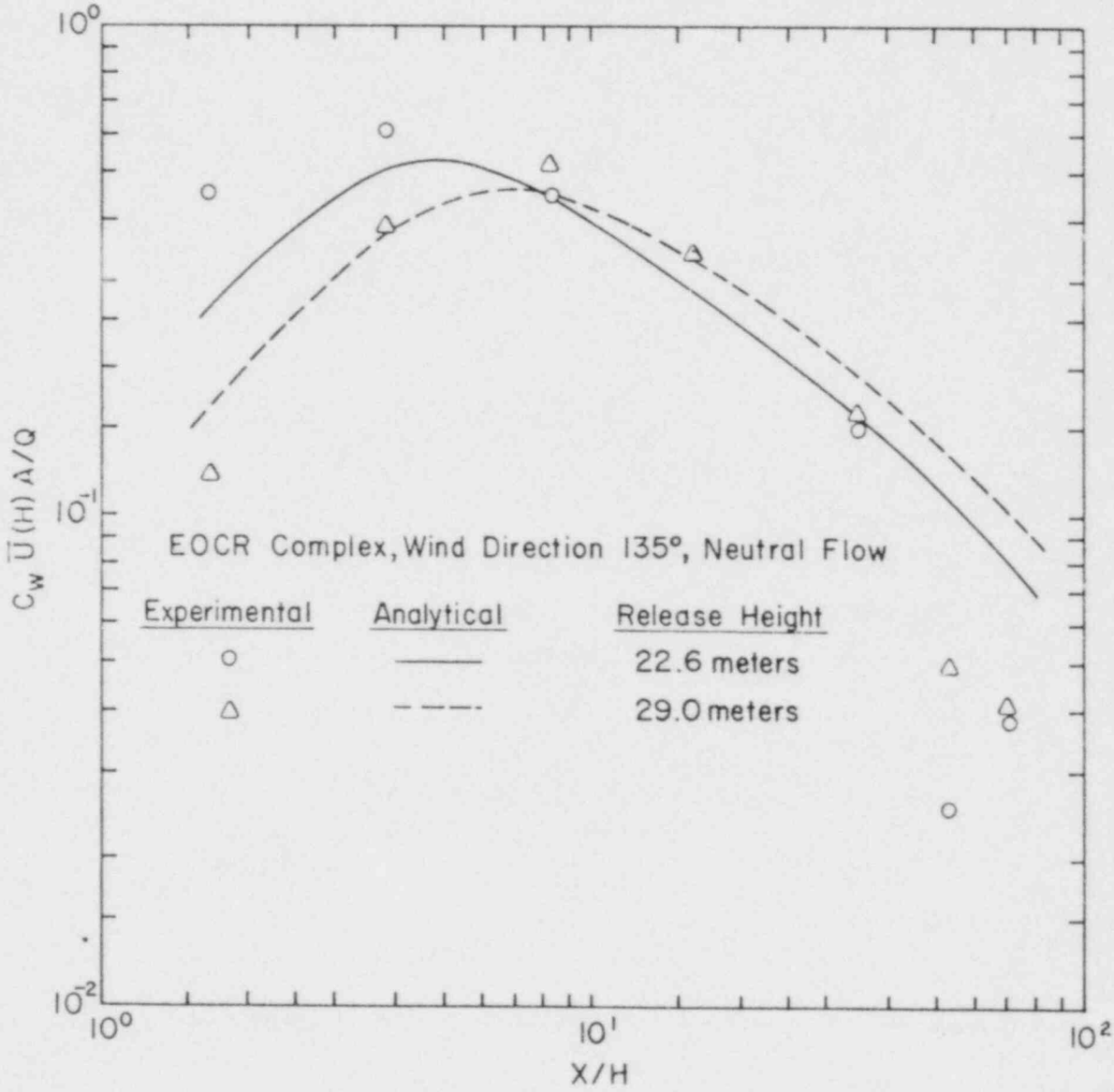

Figure 18. Comparison of ground-level concentration along the centerline of the EOCR complex with the present perturbation theory.

NRC FORM 335 (7-77)

U.S. NUCLEAR REGULATORY COMMISSION

BIBLIOGRAPHIC DATA SHEET

1. REPORT NUMBER *(Assigned by DDC)*
NUREG/CR-1473

4. TITLE AND SUBTITLE *(Add Volume No., if appropriate)*
The Wake and Diffusion Structure Behind a Model Industrial Complex

2. *(Leave blank)*

3. RECIPIENT'S ACCESSION NO.

7. AUTHOR(S)
K.M. Kothari, J.A. Peterka, and R.N. Meroney

5. DATE REPORT COMPLETED
MONTH October YEAR 1981

9. PERFORMING ORGANIZATION NAME AND MAILING ADDRESS *(Include Zip Code)*
Department of Civil Engineering
Colorado State University
Fort Collins, Colorado 80523

DATE REPORT ISSUED
MONTH November YEAR 1981

6. *(Leave blank)*

8. *(Leave blank)*

12. SPONSORING ORGANIZATION NAME AND MAILING ADDRESS *(Include Zip Code)*
Division of Health, Siting and Waste Management
Office of Nuclear Regulatory Research
U.S. Nuclear Regulatory Commission
Washington, DC 20555

10. PROJECT/TASK/WORK UNIT NO.

11. CONTRACT NO.
FIN B5829
NRC-04-76-236

13. TYPE OF REPORT
technical

PERIOD COVERED *(Inclusive dates)*

15. SUPPLEMENTARY NOTES

14. *(Leave blank)*

16. ABSTRACT *(200 words or less)*

The mean velocity, turbulence intensity and turbulent diffusion behind a model of the EOCR complex deeply submerged in a neutral turbulent boundary layer, have been investigated using wind tunnel tests and mathematical analysis. The effects of the momentum-type wake behind a complex are to decrease mean velocity and increase turbulence intensity. The complex geometry breaks down the horseshoe vortices, which consequently do not play an important role in determining wake characteristics. The decay rate of mean velocity defect was smaller than that of turbulence intensity excess variance. The wake was detected at a distance of x/H equal to 35 at a 5 percent mean velocity defect level. Such long wake regions are associated with the low roughness characteristics of the site.

The vertical profiles of velocity defect and maximum velocity defect rates compared very well with the analytical predictions except at y/H = -0.67. The experimental measurements of the decay rate of turbulent intersity excess variance also compared very well with that predicted by the theory. The ground-level concentration compared satisfactorily with the perturbation theory.

17. KEY WORDS AND DOCUMENT ANALYSIS

17a. DESCRIPTORS

17b. IDENTIFIERS/OPEN-ENDED TERMS

18. AVAILABILITY STATEMENT
Unlimited

19. SECURITY CLASS *(This report)*
Unclassified

21. NO. OF PAGES

20. SECURITY CLASS *(This page)*
Unclassified

22. PRICE
$

NUREG/CR-1473

THE WAKE AND DIFFUSION STRUCTURE BEHIND A MODEL INDUSTRIAL COMPLEX

NOVEMBER 1981